PROBABILISTIC-BASED DESIGN FACTOR FOR THE ELASTIC MODULUS OF A PULTRUDED COMPOSITE MATERIAL REINFORCED WITH A 3D BRAIDED PREFORM

By

JUAN A. ROMÁN PAGÁN

A thesis submitted in partial fulfillment of the requirements for the degree of

MASTER OF ENGINEERING

In

CIVIL ENGINEERING

UNIVERSITY OF PUERTO RICO
MAYAGUEZ CAMPUS
May, 2005

Approved by:

Arsenio Cáceres, Ph.D. Member, Graduate Committee	Date
Miguel A. Pando, Ph.D. Member, Graduate Committee	Date
Felipe J. Acosta, Ph.D. Chairman, Graduate Committee	Date
Pablo Cáceres, Ph.D. Representative of Graduate Studies	Date
Ismael Pagán Trinidad, M.S. Department Director	Date

DEDICATORY

The author wishes to dedicate this work to his family, his father Juan A. Roman, his mother Gloria E. Pagan, and sisters Vanessa Roman and Melissa Roman. They were always the principal reason for him to keep working and for bringing him an unconditional support. They were part of his growth, not only in the educative area, also in the social and moral aspects. They will always be part of his success and his live.

ACKNOWLEDGEMENTS

The author wishes to thank Dr. Felipe J. Acosta for his guidance during the development of this research. Also, he wants to thank the graduate committee members: Dr. Arsenio Cáceres, and Miguel A. Pando for their support and advice to the final document.

The author is completely grateful for the financial aid provided by the University of Puerto Rico and PR-NSF-EPSCoR start-up funds program during the development of this research.

The author also wishes to thank Mr. Elvis Ramos and Mr. Ivan Santiago for their technical support in the sample and testing set-up. He also wants to thank his class mates and structural laboratory partners for their comments and ideas across the research details.

More than anything, the author wants to thank his family and friends from his home town Jayuya, because they were always worried and proud of his success and his falls, and they were always around to keep him in the path of his goals in live.

ABSTRACT

This work describes research aimed to probabilistically assess the mechanical properties of a pultruded fiber-reinforced polymer (FRP) reinforced with a 3D braid and roving. In addition, reliability-based reduction factors for the design of such materials are developed and proposed. Elastic moduli are investigated because the design of most civil engineering applications is dominated by serviceability and buckling limit states rather than the strength. To posses a certain level of confidence in these value estimation, it is necessary to fully explode the material applications. This methodology combines simplified classical lamination theory in one case and a 3D model (Fiber Inclination Model) for braid preform in another case with experimental values in a probabilistic model to simulate the randomness of the system by the Monte Carlo technique. The accuracy of the theoretical model is investigated, evaluating the coupling effect caused by the variations in contituents and fiber orientation. Randomness is considered beginning at the micromechanical level (fiber/matrix) up to the macromechanical level (ply mechanics). All fibers were E-glass embedded in vinyl ester matrix. Reduction factors for the material are suggested providing at least a 95 % confidence level. Parametric analysis were performed evaluating the effect in the material properties by a variation of the mechanical properties (E_f, E_m) at micromechanical level, the fibers orientation (θ), and the fiber volume fraction (v_f). The proposed reduction ϕ factors for the stiffness design of the pultruded material reinforcement with a 3D braided textile are ϕ_x= 0.50 and ϕ_y= 0.75. The parametric analysis indicated that the fiber orientation and the fiber volume fraction are the variables that mostly control the variability of the material.

RESUMEN

Este trabajo describe la intención de la investigación para evaluar probabilísticamente las propiedades mecánicas de un polímero reforzado con fibras, reforzados con trenzado en 3 dimensiones y fibras paralelas en una dirección. En adición, factores de reducción para servicio para el diseño de estos materiales han sido desarrollados y propuestos. Los módulos son investigados debido a que en muchos de las aplicaciones en ingeniería civil el diseño es controlado por el nivel de servicio y limites de pandeo, más que por la capacidad. Para adquirir un cierto nivel de confianza al estimar estos valores, es necesario explotar totalmente las aplicaciones del material. Esta metodología combina la teoría de lamina clásica simplificada en un caso y un modelo de 3 dimensiones (Modelo de Fibra Inclinada) para el trenzado, a realizar en otro caso con valores experimentales en un modelo probabilística para simular la aleatoriedad del sistema por medio de la técnica de Monte Carlo. La precisión de los modelos teóricos es investigada, evaluando el efecto de acoplamiento causado por la variación en las componentes y la orientación de la fibra. La aleatoriedad es considerada empezando al nivel de la micromecánica (fibra/matriz) hasta el nivel la macro mecánica (mecánica de láminas). Todas las fibras son de vidrio tipo E, están recubiertas en resina "vinyl ester". Análisis paramétricos fueron desarrollados evaluando el efecto en las propiedades del material por una variación de las propiedades mecánicas (E_f, E_m) a nivel de la micromecánica, la orientación de las fibras(θ) y la fracción de volumen de fibra (v_f). Los factores de reducción ϕ propuestos para el diseño por servicio del material reforzado con trenzado en 3 dimensiones son ϕ_x= 0.50 y ϕ_y= 0.75. El análisis paramétrico

nos indica que la dirección de la fibra y la fracción de volumen de fibra son las variables que mayormente controlan la variabilidad del material.

TABLE OF CONTENT

TABLE OF CONTENT OF TABLES

TABLE OF CONTENT OF FIGURES

NOTATION

A_{11}	Inplane Stiffness Matrix
A_{12}	Inplane Stiffness Matrix
A_{22}	Inplane Stiffness Matrix
E_x	Modulus of Elasticity in the x-Direction.
E_y	Modulus of Elasticity in the y-Direction.
V_f	Fiber Volume Ratio
t_c	Composite Thickness
t	Thickness
P_i	Applied Load for Sample i.
A	Cross Section Area
L	Fiber Length
P_a	Unit Cell Structure Length a.
P_b	Unit Cell Structure Length b
P_c	Unit Cell Structure Length c.
H_i	Border Condition ussed in FIM
x	Sample Data Size
n	Number of Tested Samples
s	Standard Deviation
x	Sample Average
p_s	Percentile of Population
CV	Coefficient of Variation

Greek Symbols

α	Fiber Orientation used in FIM
β	Fiber Orientation used in FIM
δ	Change in any Magnitude
ε	Unit Displacement (strain)
ϕ	Capacity Reduction Factor
γ	Fiber Orientation used in FIM
μ	Unit Prefix (micro)
μ_g	Average Value for g(x) Function
θ	Fiber Orientation
ρ	Material Density
σ_g	Standard Deviation Value for g(x) Function
σ	Stress
Σ	Sum
υ	Poisson's Ratio

CHAPTER I
INTRODUCTION AND OBJECTIVES

1.1 Introduction

A Fiber-Reinforced Polymeric (FRP) material consists of a resin reinforced with a variety in form of fibers selectively oriented to achieve the desired material characteristics. Different types of fibers are available including inorganic fiber such as glass and carbon, and organic fibers such as Kevlar.

FRP's are becoming more relevant and accepted in the structural design area as a reliable material for different structural elements. This material has been used as principal structural elements in bridges and other structures. Given the fact that the strength to weight ratio is high compared to reinforced concrete and steel, it is considered an attractive alternative to retrofit existing structures.

Composite materials have been extensively used in the aerospace industry. Since the industry has great numbers of manufactures and their design tolerances are small, each design is done based on the particular application. The design guides use is mainly the Military Handbook 17. Over the last 30 years, there has been a migration from the aerospace to the construction industry. The development of composite materials as structural elements has created the necessity for research in this new type of materials. The inherent variability in FRP depends on the manufacturing processes and the material's constituents. Due to the variability of composite material properties, it is difficult to adequately evaluate its properties to fulfill the structural necessities. Also, there are many variables as the fiber volume fraction, fiber orientation and the modulus of elasticity of the

principal components that need to be considered for the design of the material. The mechanical properties, such as strength and modulus of elasticity, that control the design have to be analyzed to predict the material behavior. To have design parameter compatible with traditional civil structural design, ϕ factors for FRP must be developed to bring confidence to the property values for the structural design with this material. Because FRP design is mostly stiffness dominated (Acosta, 1999), this study will concentrate on the modus of the FRP. The determination of a reduction factor applicable to the FRP modulus of elasticity, which is the mechanical property that is studied for this project, will improve the design data with a safety range to determine the required mechanical properties of the composite.

Many analytical methods (Rule of Mixture (ROM), Fiber Inclination Model (FIM)) have been used to predict the mechanical properties of FRP materials. These formulations are based on nominal values of the different constituents, ignoring defects or variabilities in them. Formulation such a ROM, are simple and ignore complex fiber arrangement in more advanced textile. The inherent variability of FPR material at different levels (constituents and manufacturing) poses a real challenge to design engineers.

1.2 Previous Work

The FRP has been used mainly as tension resistant component bonded to concrete structural elements. Val (2003) presented the use of FRP for retrofitting of reinforced concrete columns to improve their capacity and performance. Val concluded that the capacity or FRP has to be reduced to ensure the same capacity level as the columns without confinement. Also, Ceroni, *et al*. (2004) used FRP as reinforcement material for concrete to improve the capacity and to reduce the problems that produce the failure (cracks width and

crack spacing). Ceroni prepared the specimens of concrete internally reinforced with steel bars and externally reinforced with FRP sheets. These specimens were subjected to tension test to determinate the functionality of the composite element. Based on the results, Ceroni established that the experimental failure load is lower than the theoretical expected and concluded that *"further research is necessary for the development of a more reliable formulation"*. Otherwise, Azzi and Tsai (1964) performed a comparison between theoretical modulus of elasticity and experimentally modulus of elasticity. In this case, the laminate composite consisted of a homogeneous material symmetrically oriented with an arbitrary reference angle (angle-ply). The material was exposed to tensile axial load. Azzi specified that the modulus of elasticity estimated by the Classical Lamination Theory was similar to the one determinate experimentally. Addition to these researches, Yeh and Yeh (2000), established that the mean value of axial properties in a randomly oriented laminate was closed to those values determinate by the Classical Lamination Theory. The differences between conclusions present the necessity of new research in this kind of experimental vs. theoretical comparison.

Composite materials have been manufactured assembling individual commercially manufactured sections. The actual load capacity demand for bridges has increased but the capacity of many old bridges in U.S. is less than required. Because of the necessity to improve the infrastructure capacity, FRP's have proven to be a feasible alternative. Williams, *et al.* (2003) evaluated the innovation of using FRP for bridge decks and developed experimental and analytical models to predict the behavior of the composite structure. Williams established that FRP materials fulfill the level of service required for bridges. Acosta (2002) proposed a methodology using reliability analysis to develop a design reduction factors for two types of FRP schemes for bridge decks. In his work, only

the stiffness of the material was studied because it was found that the design of FRP structures is controlled by serviceability limit states and not by strength. He established that if the variability in properties of the material could be randomized and established, the reduction factor for the modulus of elasticity of the composite could be predicted as a normal function incorporating variabilities at the constituents and manufacturing levels. Reduction factors for materials using braided preforms turned to be lower than stitched fabric laminates due to the variability in the material behavior caused by the waviness of the fibers in the braided preform and the uneven distribution of roving. The proposed reduction factor was 0.50. Also Zureick and Steffen (2000) developed a research with pultruded FRP material reinforced with unidirectional roving and continuous strands mats (CSM) as short columns exposed to compression loads. This research focused in the determination of a reduction factor for axial compression load in columns. They also used the Monte Carlo Simulation to estimate the reliability analysis to the columns samples. Zureick and Steffen (2000) concluded that the target reliability analysis in this case was "overly conservative". In other case, Lundberg and Galambos (1996) performed a randomly statistically analysis with concrete-filled tube columns samples with Monte Carlo Simulation. In this analysis they determinate the reliability index to estimate design factor for this material, but they concluded that some of the samples data that do not fulfill the reliability condition should not be used for the design factor analysis. They underpredicted the test capacity, because the test-to-prediction ratio of the reliability index were between 1.23-1.46, with a coefficient of variation of 0.14-0.25.

To determine the modulus of elasticity of FRP's, tensile and compressive tests have been performed by many researchers. Deitz, *et al.* (2003) subjected the commercially produced #15 Glass-FRP's rebar (15 mm barrel diameter) to compression static load to

develop stress-strain diagrams to determinate de modulus of elasticity and to approximate their values with analytical models. He concluded that the expected modulus of elasticity in compression could be compared and approximated as equal to the tensile modulus. Similar tests were conducted in compression and tension by Acosta (1999) where two configurations of FRP were characterized. Acosta performed static tensile test on coupons to obtain the mechanical properties of plates and triangular beams. A stress-strain diagram was developed for each coupon where the modulus of elasticity was evaluated.

As seen in the previous research, the FRP have been tested to be characterized in different ways, such as in the mechanical properties as a structural element, and a retrofitting material. The material (FRP) has a high weight to strength ratio, and corrosion and thermal resistance. Most of the common uses of the material is as reinforcement for concrete structures and is also used for space aircraft. Due to the differences in conclusions, tensile properties of the material will be analyzed for futures uses as a structural material. For that reason, the material will be tested in tension in the principal fiber directions to develop the characterization of the material and to propose design reduction factors for the modulus of elasticity.

1.3 Objectives

The literature presents that the FRP is used as a retrofit material and has been evaluated with the possibility to be developed as a structural material. The difficulty to simulate the behavior of the material mechanical properties does not give the designer the confidence to evaluate and consider the FRP as a viable alternative for construction as the classical materials (concrete, steel, and wood).

Experimentally and analytically, this project evaluates the mechanical properties of FRP consisting of a vinylester resin reinforced with an E-glass 3D braided preform. The experimental characterization will be performed by subjecting the specimens to tensile load in the longitudinal and transverse directions. Also, another goal is to develop a design ϕ factors accounting for inherent material variability at the constituents and manufacturing variables. These factors will be evaluated by a statistical data analysis of the experimental results for the modulus of elasticity.

This work expanded the research by Acosta (1999) where he performed similar mechanical tests to a limited number of samples of the same FRP. His work lacks of statistical significance which is covered in this work. This project, also, increased the possibility of generating reduction ϕ factors that will be used for future FRP design.

This work is organized as following: Chapter II presents the physical and mechanical properties and characteristics of the FRP. Chapter III presents the analytical models used to estimate the theoretical modulus of elasticity. Chapter IV shows the statistical analysis used to reduce the experimental data and to estimate the reduction factors. This Chapter also presents the analytical results and the recommended reduction

factors. Finally, Chapter V presents the conclusions of the project and recommendations for future research.

CHAPTER II

MATERIAL PROPERTIES, TEST DESCRIPTION AND EXPERIMENTAL RESULTS

2.1 Introduction

This chapter presents the physical properties (fiber type and layout, specific gravity, density, fiber content and material components) of the FRP material selected for investigation in this project. The mechanical properties (modulus of elasticity and strength) measured by the tensile tests are also presented in this chapter.

2.2 Methodology

2.2.1 Material Description

The material studied in this work is a vinylester resin reinforced with E-glass fibers in the form of a three-dimensional braided textile. Figure 2.1 shows a photograph of a dry E-glass 3D braided textile. This 3D braided textile has fibers oriented at 0˚ and at +/- θ. Detail on the manufacturing technique of the textile can be found in Brown and Crow (1992). Coupon-sized specimens are excised from triangular tubes used as the webs for an FRP bridge deck developed at Georgia Institute of Technology (Acosta, 1999). The material was tested along the principal material directions, defined in Figure 2.2. The principal directions of the material are defined based on fiber orientation. The orientation is based on the local coordinates system x-y where the fiber 0˚ direction is parallel to the local x-axis also referred as the longitudinal direction. The transverse direction is perpendicular to the longitudinal direction. E-glass roving also runs parallel to the x-direction and the 0°

orientation of the 3D braid. It was used to aid the pulling of the braid in the pultrusion process.

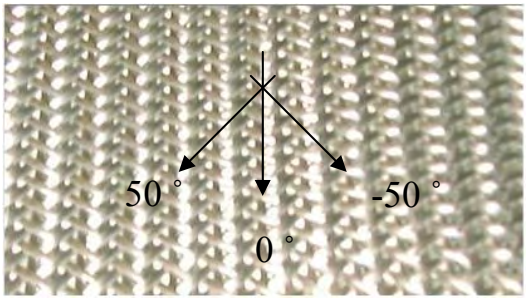

Figure 2.1: Three-Dimensional Braided Textile.

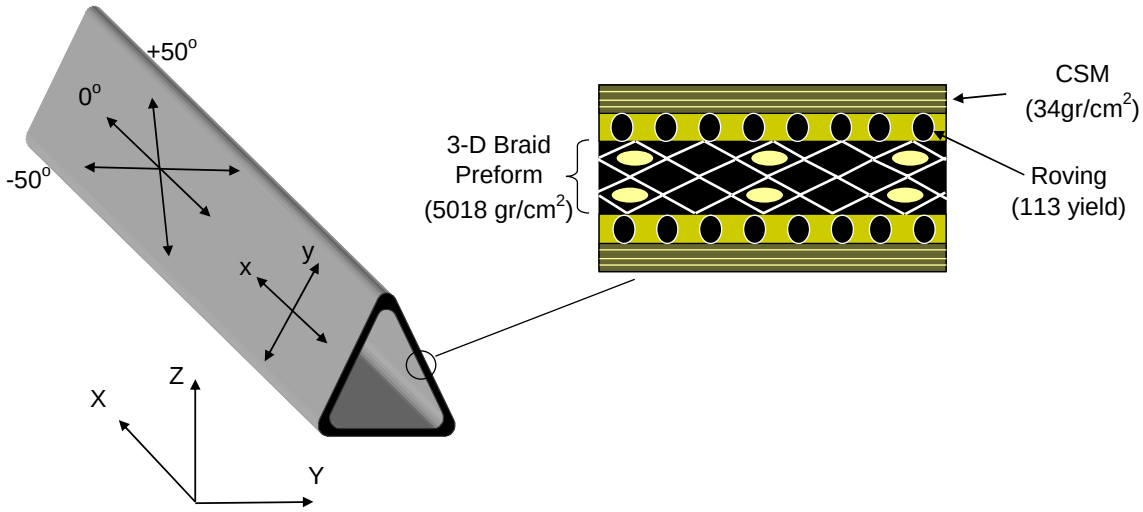

Figure 2.2: Fibers Lay -Up For the Triangular Beam and its Orientation with respect to the Triangular Beam Axes.

2.2.2 Coupons Description

The coupons were cut along the two principal directions (local x and y). The specimens cut along the x-direction have nominal dimensions of 51 mm (2 in) wide, 6 mm (1/4 in) thick, and 305 mm (12 in) long. The specimens cut along the y-direction have nominal dimensions of 32 mm (1.25 in) wide, 6 mm (1/4 in) thick, and 254 mm (10 in) long. This length is limited by the size of the cross-section. Table 2.1 reports a summary of the coupon dimensions. The statistical analyses of the dimensions of the coupons are reported in Appendix A.

Table 2.1: Nominal Dimensions of the Tensile Coupons

Test Coupons Set	Number of Samples	Width (in)		Thickness (in)		Length (in)	Average Area (in^2)
		Minimum	Maximum	Minimum	Maximum		
1	30	2.041	2.082	0.205	0.243	12.00	0.4639
2	30	1.230	1.580	0.230	0.250	7.25	0.3031

Deformations were measured by strain gauges in a limited numbers of coupons. The rest of the coupons were instrumented with a strain gage extensometer as show in Figure 2.3. The applied load was also recorded to compute the stress level through each test.

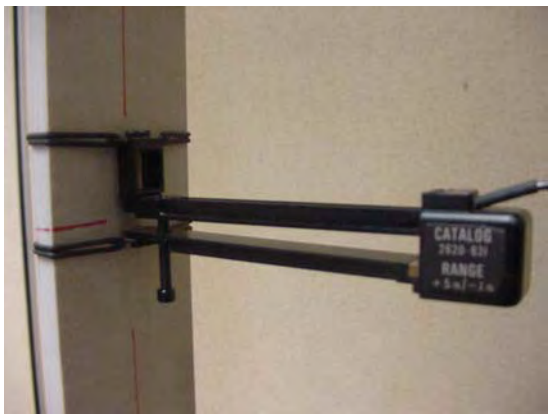

Figure 2.3: Location of the Strain Gage Extensometer.

The fiber lay-up is also presented in Figure 2.2, which shows the space between the roving, the total wall thickness, and the dry weight of each E-glass constituents of the reinforcement. Figure 2.4 presents a microscope picture of the material. This picture shows how the continuous strand mats (CSM), roving and 3-D braid are lay-up. The braid has fibers oriented in three directions [0°, +50°, -50°] where the 0˚ is parallel to the x-direction of the tubes.

Table 2.2 presents the physical characteristics considered in the analysis of this composite (Acosta, 1999). Table 2.3 presents the mechanical properties of the materials used to estimate the mechanical characteristics of the composite. The analysis will consider a variation in the orientation angle of the braid and in the modulus of elasticity of the fiber and the matrix. This variation will consider the manufacture variabilities of the material. To perform the analysis, a 5% variation of the nominal value of the properties will be used for the variation as presented in Table 2.3.

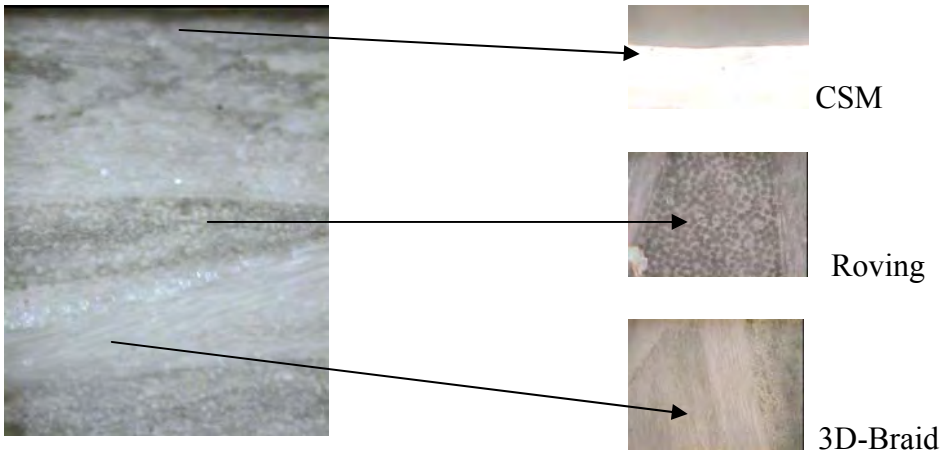

(a) **(b)**

Figure 2.4: Microscope Picture of (a) Part of the Samples Cross- Section (b) Specific Zoom of Each Fiber.

Table 2.2: Physical Characteristics of the Material

Material	Physical Characteristics			
	Density	Fiber Volume Ratio (V_f)	Thickness (t_c, in)	Fiber Orientation (Degree)
Roving	113 yield	0.208	0.0502	0
CSM	34 gr/cm^2	0.031	0.0316	0
3-D Braid	5018 gr/cm^2	0.464	0.0381	-50
	5018 gr/cm^2	0.464	0.0381	50
	5018 gr/cm^2	0.464	0.0762	0

Table 2.3: Nominal Mechanical Characteristics of the Material from Literature (Barbero, 1998)

Material	Fiber Mechanical Characteristics	
	Poisson's ratio (ν)	Modulus of Elasticity (Ksi)
E-Glass Fiber	0.25	10500
Vinyl Ester Resin	0.22	500

Coupon-sized specimens were tested in tension along the longitudinal and transverse directions, where load and deformations were measured. Tests were loaded in displacement control at a rate of 2 mm per minute (0.05 in/min), as established by *ASTM D 3039*.

2.2.3 Tensile Test Description

Mechanical characterization of the composite material are evaluated by performing a series of tensile tests with the material oriented at its principal directions. Due to the fiber nature of the material, results are also affected by the type of load (tension and compression). Tensile tests were performed on the material to determine its elastic modulus and strength under each type of loading. The axial deformations were measured using the extensometer attached to the sample surface. A load cell attached to the MTS frame was used to record the applied load. Stresses (σ_i) are computed dividing the applied load (P_i) by the sample cross-sectional area (A), where i is the data number for the applied load, expressed as:

$$\sigma_i = \frac{P_i}{A} \tag{2.1}$$

For the determination of the engineering modulus of elasticity of the material, the parameter established by the *ASTM D 3039* was used and the chord modulus was determined between 1000 and 3000 microstrain *($\mu\varepsilon$)* (Range 1). Also the initial tangent modulus was computed from strain values between 0 and 1000 microstrain *($\mu\varepsilon$)* (Range 2). The modulus of elasticity can be obtained using the expression:

$$E^{chord} = \frac{\Delta\sigma}{\Delta\varepsilon} \tag{2.2}$$

where the stress is divided by the strain between the ranges established by the *ASTM* standard. Due to the variability behavior of the material during the testing, the modulus of elasticity was determined applying linear regression to the stress-strain data.

The modulus of elasticity was determined in each direction. The longitudinal modulus was obtained with the load applied parallel to the principal direction and the transverse modulus was similarly obtained, but with the load applied perpendicular to the principal orientation as shown in Figure 2.5.

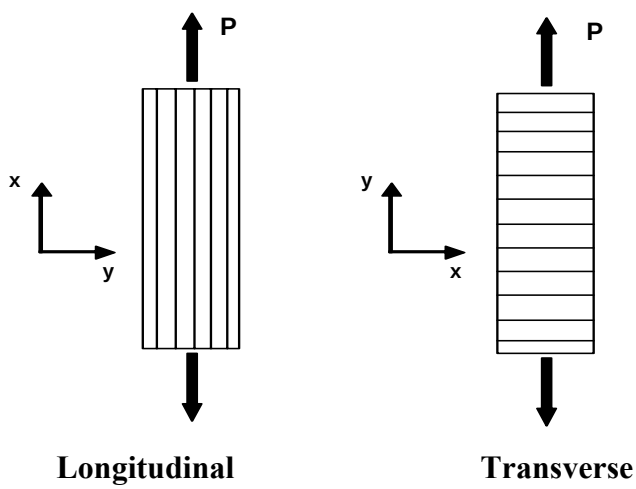

Figure 2.5: Load and Fiber Orientation for the Modulus of Elasticity.

2.2.3 Tensile Modulus of Elasticity of Tested Coupons.

Tensile tests in the two principal directions were performed on a total of 60 coupons, 30 for each direction. From each test, stress-strain diagrams similar to the one shown in Figures 2.6 were generated to determine the modulus of elasticity of the composite. Stress-Strain curves for all coupons are reported in Appendix B. The graph shows two values of modulus. One was from data of *Range 2*. The second was from *Range 1* as established in the *ASTM D 3039*. Both moduli were computed applying linear

regression to the data points in their respective ranges. Descriptive statistics of the experimental data are discussed in Chapter 4.

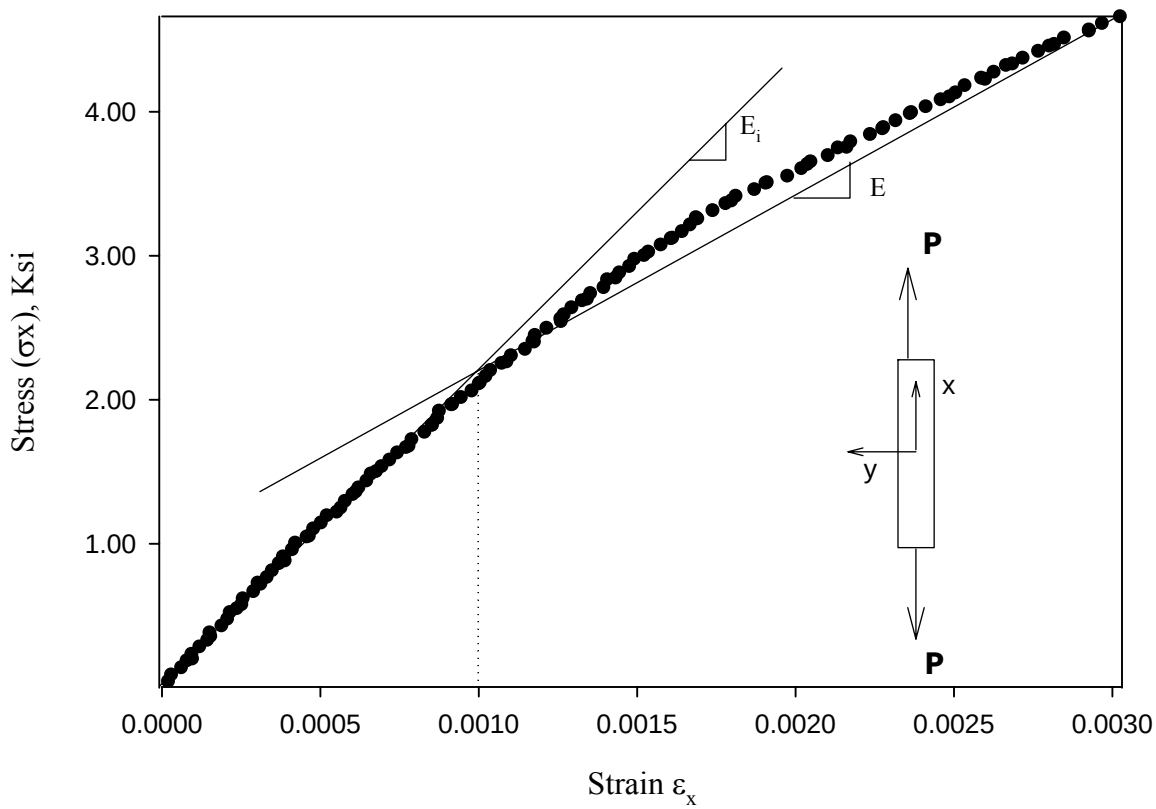

Figure 2.6: Portion of a Typical Stress- Strain Curve for Coupons in the longitudinal Direction.

Figures 2.7, 2.8, and 2.9 shows the stress-strain diagrams for the tested coupons in the principal direction and in the transverse direction respectively. These figures present how the sample data are close one with each other at a close range. The variability in the experimental data shown in the figure can be caused by different reasons. These reasons could be slipping of the samples in the grips during the test, stress concentration and also the slip of the extensometer in the sample surface. Also the micro cracks (microscopic failures due to the fabrication process) in the material, the bonding between the fiber and the resin, and the change in temperature could present variation in the material behavior during the test.

Figure 2.10(a) shows how an FRP with a 3D braid looks at failure. This failure could be compared with the one shown in Figure 2.10(b) which is of a composite with reinforcement of fiber in a weave form. In the Picture of the FRP with a 3D braid can be seen that the fiber keep the plies together even though the resin failed. Delamination is prevented by the through-the-thickness reinforcement provided by the 3D structure. Failure of the FRP with the weave reinforcement showed heavy delamination of the layers because of the lack of through-the-thickness reinforcement.

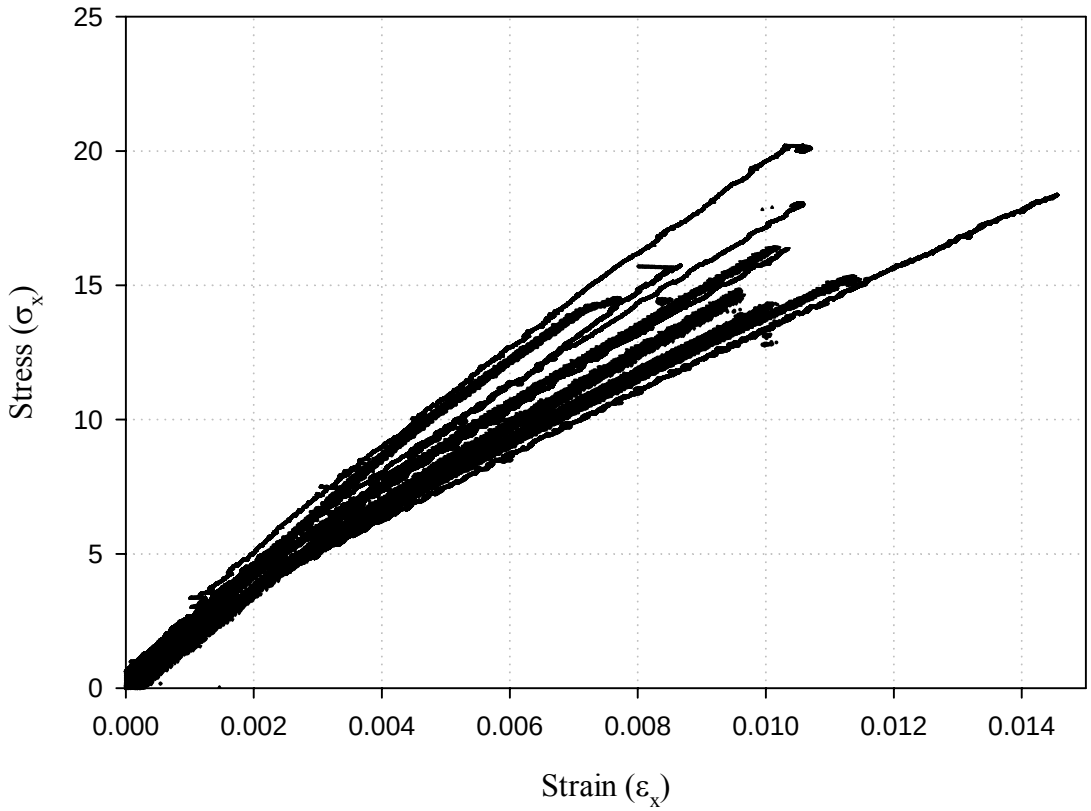

Figure 2.7: Total Portion to Failure of a Typical Stress- Strain Curves for Coupons in the Longitudinal Direction.

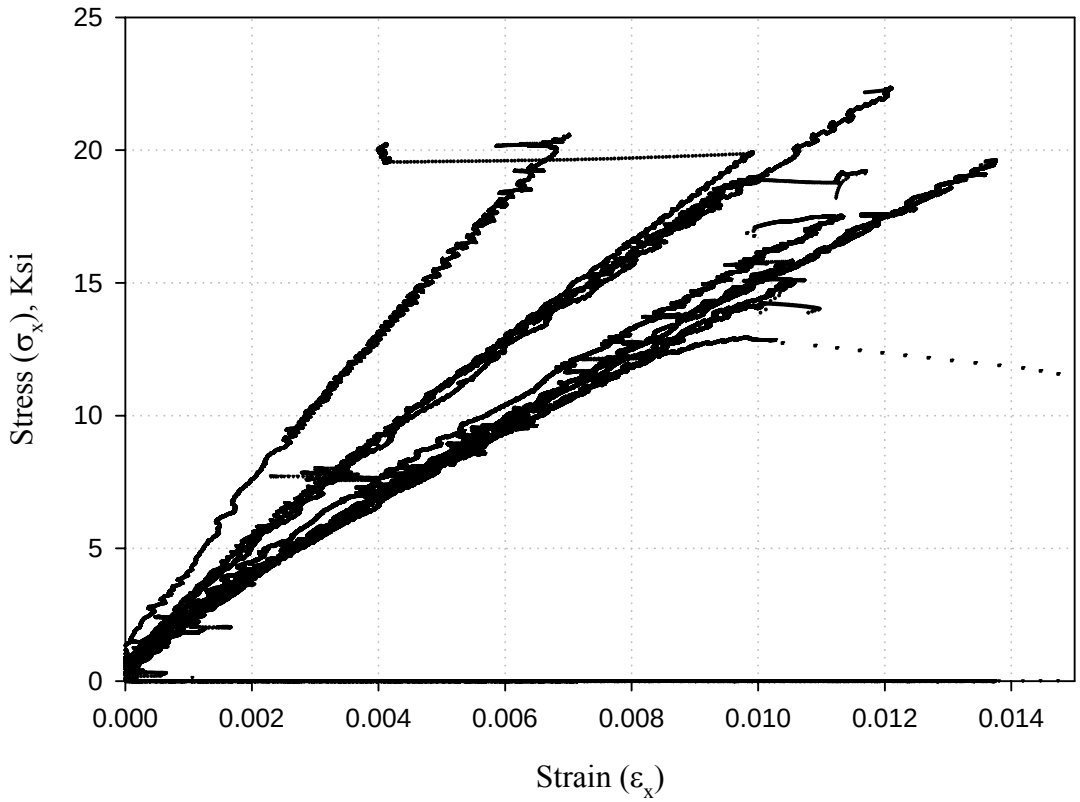

Figure 2.8: Total Portion to Failure of a Typical Stress- Strain Curve s for Coupons in the Longitudinal Direction.

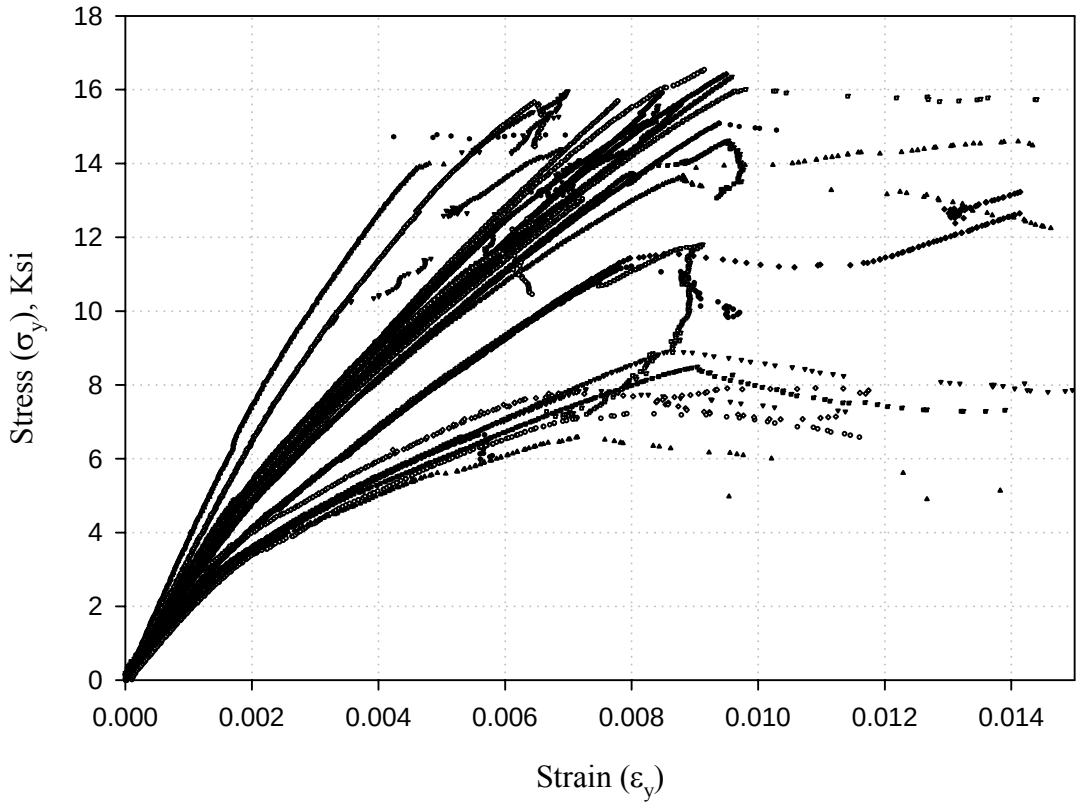

Figure 2.9: Total Portion to Failure of a Typical Stress- Strain Curves for Coupons in the Transverse Direction.

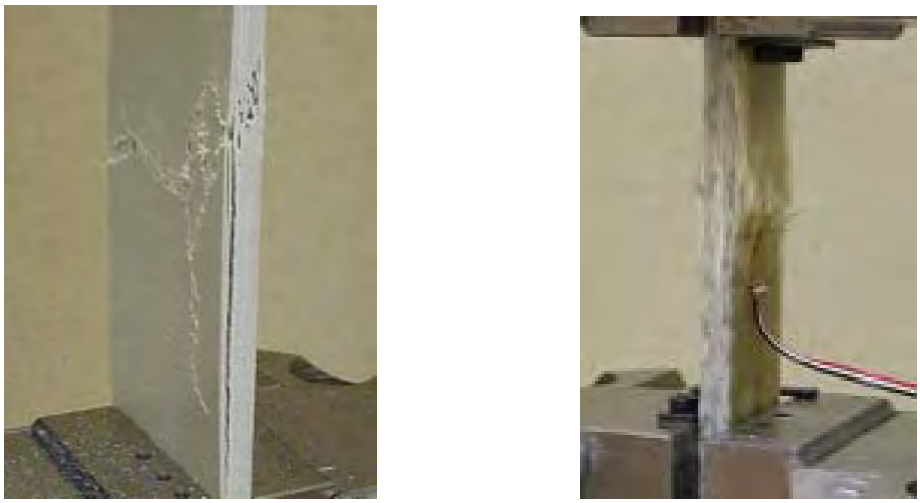

(a) (b)

Figure 2.10: Failure Mode: (a) FRP with 3D Braids (b) FRP with Weave Fiber Form.

In addition, tensile tests were performed using the extensometer and strain gages to estimate the strain of the material. Figure 2.11 present how the strain was recorded with both strain gage devices. The figure shows the comparison of the strains recorded with the extensometer and the strain gage against applied stress. This results show that with any of those two devices the strain was correctly recorded. This analysis can eliminate the possibility that the extensometer could slid in the surface of the material during the test.

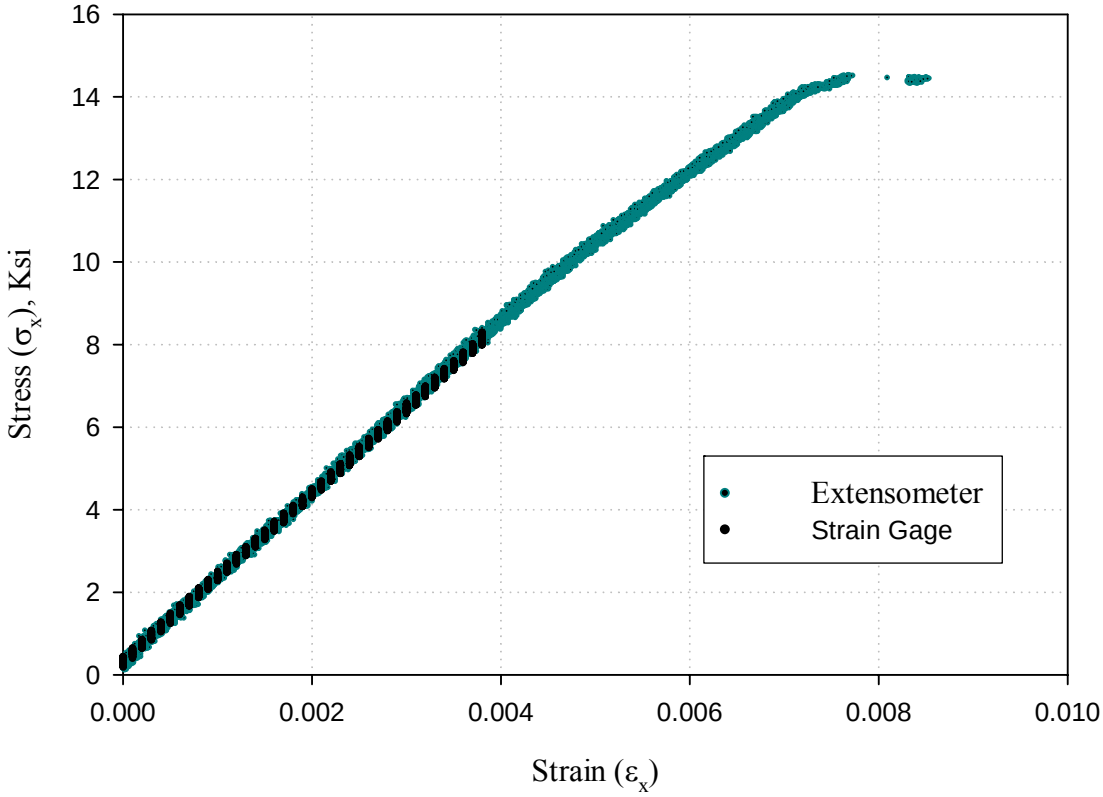

Figure 2.11: Comparison of Responses Measured with Strain Gage and Extensometer.

2.3 Experimental Results

The experimental modulus of elasticity for each tested coupon in both directions is reported in Table 2.4. Table 2.5 reports the descriptive statistics of the tested coupons. The table includes the average values of strength and modulus of elasticity, coefficient of variation, and standard deviation.

In Table 2.4, the values in bold are outliers detected by the statistical analysis. These values represent the data points that are outside suspiciously too high or too low of the majority of the values of the population. The outlier values were removed from the data following methodology in the *ASTM D 3039* and the Military Handbook 17 to perform the statistical analysis again and improve the precision of the results.

Table 2.4: Experimental Results for Modulus of Elasticity.

Number of Coupon	E_i [ksi (GPa)] ($0<\varepsilon<0.001$)		E [ksi (GPa)] ($0.001<\varepsilon<0.003$)	
	Longitudinal	**Transverse**	**Longitudinal**	**Transverse**
1	2143 (14.78)	2301 (15.87)	1884 (13.00)	1166 (8.04)
2	1863 (12.85)	2017 (13.91)	1735 (11.97)	1155 (7.97)
3	1614 (11.13)	2102 (14.50)	1428 (9.85)	1229 (8.48)
4	2249 (15.51)	1901 (13.11)	2205 (15.20)	1287 (8.88)
5	1853 (12.78)	2160 (14.89)	1568 (10.81)	1146 (7.90)
6	2103 (14.58)	2277 (15.71)	1714 (11.82)	1546 (10.66)
7	2077 (14.32)	3461 (23.87)	1881 (12.97)	3256 (22.45)
8	1484 (10.23)	2152 (14.84)	1344 (9.27)	1601 (11.04)
9	**3456 (23.84)**	2477 (17.09)	**2897 (19.98)**	1160 (8.00)
10	2449 (16.89)	2171 (14.97)	2045 (14.10)	1014 (7.00)
11	1758 (12.12)	**3871 (26.70)**	1517 (10.46)	3195 (22.04)
12	2282 (15.74)	2451 (16.90)	2019 (13.92)	1973 (13.60)
13	2253 (15.53)	2671 (18.42)	1610 (11.10)	2272 (15.67)
14	2329 (16.06)	2564 (17.68)	2072 (14.29)	2060 (14.21)
15	1747 (12.05)	2822 (19.46)	1606 (11.07)	2206 (15.21)
16	1625 (11.21)	2576 (17.77)	1588 (10.95)	2203 (15.20)
17	1890 (13.04)	2661 (18.35)	1694 (11.68)	2033 (14.02)
18	1804 (12.44)	2732 (18.84)	1538 (10.60)	2095 (14.45)
19	2052 (14.15)	2644 (18.24)	1654 (11.41)	2116 (14.60)
20	1936 (13.35)	2682 (18.50)	1570 (10.83)	2029 (13.99)
21	1832 (12.63)	3269 (22.55)	1637 (11.29)	2894 (19.96)
22	2772 (19.12)	2642 (18.22)	**3044 (20.99)**	1938 (13.37)
23	1787 (12.32)	2639 (18.20)	1639 (11.30)	2118 (14.60)
24	1755 (12.10)	2722 (18.77)	1706 (11.77)	2012 (13.88)
25	1801 (12.42)	2630 (18.14)	1583 (10.92)	2087 (14.39)
26	1860 (12.83)	2206 (15.21)	1746 (12.04)	1570 (10.83)
27	2079 (14.34)	2822 (19.46)	2064 (14.23)	2137 (14.74)
28	2018 (13.92)	2745 (18.93)	1759 (12.13)	2062 (14.22)
29	2206 (15.21)	2991 (20.63)	1762 (12.15)	2124 (14.65)
30	1952 (13.46)	2613 (18.02)	1533 (10.57)	1888 (13.02)

* Outliers removed for statistical calculations.

Table 2.5: Statistics of Tested Coupons without Outliers.

	Longitudinal			Tranverse		
	Average	Std. Dev.	C.V. (%)	Average	Std. Dev.	C.V. (%)
Strength ksi (MPa)]	16.7 (115.37)	3.4 (23.25)	20.1	8.40 (57.93)	0.65 (4.48)	7.8
Modulus [ksi (GPa)] 0 - 0.001	1985 (13.69)	278 (1.92)	14.0	2555 (17.62)	354 (2.44)	13.9
Modulus [ksi (GPa)] 0.001 - 0.003	1718 (11.85)	210 (1.45)	13.8	1919 (13.24)	567 (3.91)	29.5

CHAPTER III
ANALITYCAL MODELS FOR THE MODULUS OF ELASTICITY

3.1 Introduction

This chapter presents the analytical methods used to approximate the nominal value of the modulus of elasticity of the material. The methodology presented in this chapter includes the well known Classical Lamination Theory and the Rule of Mixture and the no so common Fiber Inclination Model developed for 3D textiles.

3.2 Model Description

Prediction of the modulus of elasticity was performed using two analytical methods. These are the well known Classical Lamination Theory (CLT) and Fiber Inclination Model (Chou, 1992). The Rule of Mixture (ROM) was used to calculate the principal stiffness values of each lamina. The CLT estimate the theoretical value for the modulus of elasticity or as sometimes known as the engineering modulus in both directions (longitudinal (E_x) and Transverse (E_y)), For a symmetric and balanced laminate, the in-plane moduli are:

$$E_x = \frac{1}{t\alpha_{11}} = \frac{A_{11}A_{22} - A_{12}}{tA_{22}}$$
$$E_y = \frac{1}{t\alpha_{22}} = \frac{A_{11}A_{22} - A_{12}}{tA_{11}} \tag{3.1}$$

where A_{ij} $(i\ ,j= 1, 2, 6)$ are the in-plane stiffness matrices of a laminate, and t is the total laminate thickness. The [A] matrix depends on the material mechanical and physical properties (E_f, E_m, V_f, ν_f, ν_m,, ρ_c, *etc.*) and the lamina orientation. For nominal moduli, fixed values of the properties are used. Nominal values are reported in Table 2.2 and Table 2.3

taken from the literature (Barbero, 1998). These values were determined, according to the directions of each layer, and physical properties of the materials. Randomly generated laminate properties are used to determinate design constant. To estimate these values, the mechanical and physical properties as the fiber volume ratio, modulus of elasticity of the fiber and the matrix, Poissson's ratio and density are used without varying the average value with the standard deviation. These are presented in detail in the next chapter.

The Fiber Inclination Model (FIM) (Chou, 1992) was developed considering a unit cell structure (smallest particle containing all the material properties). A schematic representation of the used unit cell of this study is shown in Figure 3.1. The figure presents the cell dimensions, the coordinate system and the fiber orientations used in the analysis. The FIM considers the in-plane stiffness matrices as an integration of the characteristic matrices using the fiber layer thickness in the unit cell structure. The parameters of the integration are based on the dimension of the unit cell structure and the fiber volume ratio (v_f) in each direction, which is assumed to be the same of the composite. The expressions for the geometry configurations of the lamina are presented in Equation 3.2 as a function of the fiber length, thickness variation (φ) and the thickness of the cell (P_c), where $L = \sqrt{P_a^2 + P_b^2}$, P_c is the unit cell thickness and ε_i is the length variation of the unit cell structure.

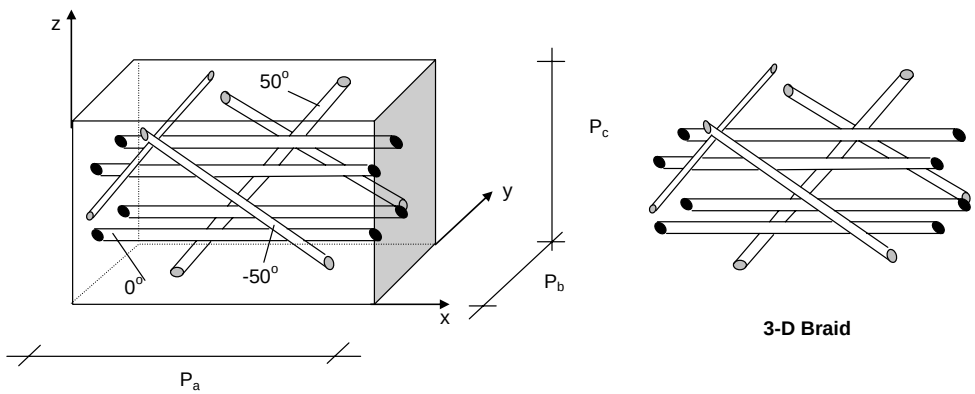

Figure 3.1: Unit Cell Structure and 3-D Braid Configuration.

$$
\begin{aligned}
H1 &= \frac{P_c \varphi_1}{L} \\
H2 &= \frac{P_c \varphi_2}{L} \\
H3 &= P_c \left(\frac{1-\varphi_1}{L} \right) \\
H4 &= P_c \left(\frac{1-\varphi_2}{L} \right)
\end{aligned}
\tag{3.2}
$$

The yarn orientation is represented by the angles α, β and γ. These angles represent the fiber orientation in the unit cell structure and will be considered estimating the in-plane stiffness matrices for the inclined fibers.

The α, β and γ angles are determined using the Equations (3.3) as a function of the unit cell dimensions. These are:

$$
\begin{aligned}
\alpha &= \tan^{-1}\left(\sqrt{\frac{P_a^2 + P_b^2}{P_a}} \right) \\
\beta &= \tan^{-1}\left(\frac{P_b}{P_a} \right) \\
\gamma &= \tan^{-1}\left(\frac{P_c}{L} \right)
\end{aligned}
\tag{3.3}
$$

The stiffness of the material was evaluated using the constitutive equations similar to the CLT model. The orientation of the fiber was considered to estimate the stiffness of the composite with the thickness of each lamina using the Equation 3.4 (Chou, 1992).

$$A_{ij}(x) = \int_{H_1(\xi_1)}^{H_1(\xi_1)+h'} \overline{Q}_{ij}^{(1)}(\beta,\gamma)dz + \int_{H_2(\xi_2)+h'}^{H_2(\xi_2)} \overline{Q}_{ij}^{(2)}(\beta,\gamma)dz + \int_{H_3(\xi_1)}^{H_3(\xi_1)+h'} \overline{Q}_{ij}^{(3)}(\beta,\gamma)dz + \int_{H_4(\xi_2)+h'}^{H_4(\xi_2)} \overline{Q}_{ij}^{(4)}(\beta,\gamma)dz \qquad (3.4)$$

where $h' = h/(\cos\gamma)$, and h is the thickness of each lamina. The reduced stiffness matrix (Q) depends on the constituent's properties $(E_f, E_m, \nu_f \text{ and } \theta)$ in each ply. The sign of the β and γ depend on the orientation of the fiber layers. To simplify the analysis of the composite, the distribution of the thickness of the braid part was defined in this case each fiber orientation as $h_0 = h_{braid}/2$, $h_{50} = h_{braid}/4$, $h_{-50} = h_{braid}/2$, where h_0 is the thickness of the lamina orientated at 0°, h_{50} for the lamina orientated at 50° and h_{-50} for the lamina orientated at -50° and h_{braid} is the thickness of the 3-D braid as presented in Figure 2.4. Table 3.1 reports computed nominal values of the Moduli for both methods. Results show considerable difference between both methods along the x-direction. This difference can be attributed to the simplification of the material lay-up for the CLT model and the variation of the fibers orientation respecting to the unit cell dimensions for the FIM model.

Table 3.1: Nominal Values of Modulus of Elasticity

Method	Ex [ksi (Gpa)]	Ey [ksi (Gpa)]
Classical Lamination Theory	2640 (18.20)	1246 (8.59)
Fiber Inclination Model	2895(19.97)	1281 (8.84)

CHAPTER IV
RELIABILITY DESIGN FACTOR AND STATISTICAL ANALYSIS

4.1 Introduction

This chapter presents the application of the Classical Lamination Theory and Fiber Inclination Model combined with the experimental data incorporated into the reliability based model to determinate the design factor for the FRP with statistical analysis.

4.2 Descriptive Statistics

The method used to analyze the experimental data followed the procedure included in the *ASTM D 3039* Standard. The statistical analysis consisted on determining the average value ($\bar{x}$), standard deviation (s), and coefficient of variation (CV), which expressions are shown in Equations 4.1, 4.2, and 4.3 respectively. The x_i represents each of the experimental data values and n is the number of samples.

$$\bar{x} = \frac{x_1 + x_2 + \ldots + x_n}{n} = \frac{1}{n}\sum_{i=1}^{n} x_i \tag{4.1}$$

$$s = \sqrt{\frac{1}{n-1}\sum_{i=1}^{n}(x_i - \bar{x})^2} \tag{4.2}$$

$$CV = \frac{s}{\bar{x}} \times 100 \tag{4.3}$$

4.3 Reliability- Based Analysis

To determinate the reduction factor for the mechanical properties of the composite, a statistical and probabilistic analysis was developed. To have reasonable statistical analysis, 30 samples were tested in each of material directions previously established for a

total of 60 samples. To generate random analytical values, the well known Monte Carlo Simulation was used. The randomly generated values simulate the inherent variability of the material. This simulation results in random values of the theoretical modulus of elasticity. This simulation was performed using commercially available software. In order to find the design factor that provides enough confidence for design, the performance function *g(x)* was defined, wich expression is;

$$g(x) = E^{\exp} - E^{pred} \tag{4.4}$$

This expression represents the differences between the experimental modulus (E^{exp}) and the predicted modulus ($E^{pred} = \phi E^{th}$) generated. This predicted modulus includes the randomly generated theoretical values multiplied by the design ϕ factor that will be varied to achieve certain confidence level. This function is assumed to have normal variation with average value (μ_g) and standard deviation (σ_g). The shaped area represents an allowable risk to the material to fault the required material stiffness.

The analytical and experimental moduli used for analysis of Equation 4.4 are reported in Table 4.1 and Table 4.2. The analytical and experimental values of the modulus of elasticity in each direction (E_x and E_y) used in the analysis are reported in Table 4.1 and Table 4.2 respectively. The experimental moduli values in both directions are reported in the table corresponding to *Range 1*. Figure 4.2 and Figure 4.3 present the comparisons between the modulus shown in Table 4.1 and 4.2 respectively. These values were randomly and normally distributed. Figures 4.2 and 4.3 shows the modulus of elasticity for CLT and FIM models respectively.

Figure 4.4 shows the safety factor effect of the reduction factor that will be proposed for design of this composite material. The values plotted in the figure represent

the normally distributed experimental data compared with analytical stiffness estimated from CLT in the x-direction. The distribution functions that correspond to these simulations are shown in Figures C.1, C.2, C.3, and C.4 of Appendix C.

The curve for E^{pred} in Figure 4.4 and Figure 4.5 were computed using ϕ= 0.59 for the x-direction and ϕ= 0.76 for the y-direction for the CLT respectively. To predict the reduction ϕ factor, β have to be considered to determine the percentile of the performance function *g(x)*. This reliability index β represents the relation between the average and the standard deviation of the performance function *g(x)*, as presented in Equation 4.5, where μ_g is the average value and σ_g is the standard deviation. The probability of success, p_s, is a function of β which expression is shown in Equation 4.6. Here $\Phi(-\beta)$ is the cumulative distribution function for normal distribution.

$$\beta = \frac{\mu_g}{\sigma_g} \tag{4.5}$$

$$p_s = 1 - \Phi(-\beta) > 0.95 \tag{4.6}$$

To estimate the reduction factor for each direction (x, y), the Equation 4.6 was analyzed varying ϕ between 0.45 to 1.0 to determine the value that makes Equation 4.6 true. The cumulative curve that represents the behavior of the Equation 4.6 is shown in Figure 4.6. The data shown in the figure is for a performance function where the percentile of the population (p_s) is greater than 95 %. To determinate the exact ϕ factor value, the desired percentile is 95%.

The same procedure was repeating using the Eth from the FIM model. The curves of the stiffness reduction factor are shown in Figure 4.6 and 4.7. These figures were developed using reduction factors of ϕ= 0.53 and ϕ= 0.75 for the x-direction and the y-direction for the FIM model respectively. The frequency distribution and cumulative distribution that represent the analysis with this method are presented in Figures C.5, C.6, C.7, and C.8 in Appendix C.

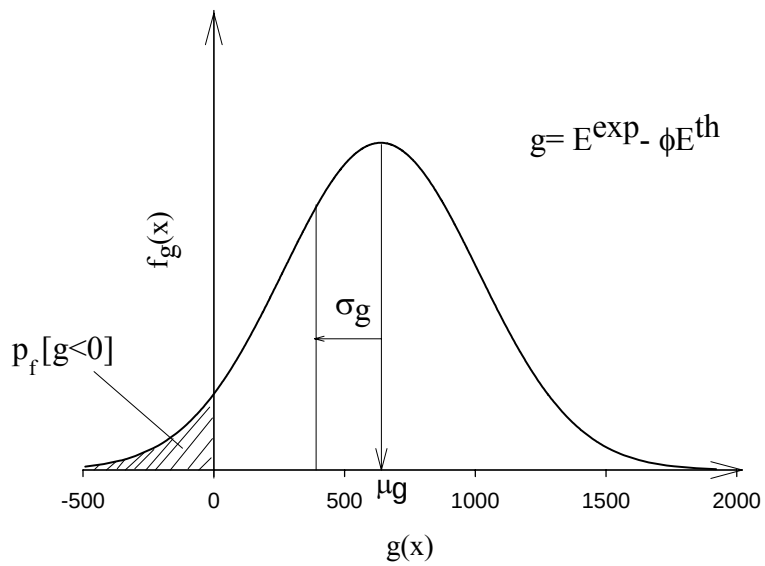

Figure 4.1: Probability Distribution of the Performance Function *g*.

Table 4.1: Modulus of Elasticity in the x- Direction.

Method	Ex [ksi (GPa)]	Standard Deviation	CV (%)
Classical Lamination Theory	2508 (17.30)	187 (1.29)	7.4
Fiber Inclination Model	2878 (19.85)	158 (1.09)	5.5
Experimental Average Result	1718 (11.85)	210 (1.45)	13.8

Table 4.2: Modulus of Elasticity in the y- Direction.

Method	Ey [ksi (GPa)]	Standard Deviation	CV (%)
Classical Lamination Theory	1215 (8.38)	142 (0.98)	11.7
Fiber Inclination Model	1290(8.90)	140 (0.97)	10.9
Experimental Average Result	1919 (13.24)	567 (3.91)	29.5

The performance function *g(x)* for the CLT model is presented in Figure 4.8. This figure shows a curve of real data of the behavior of the Equation 4.6. In that figure it can be appreciated that the average value of the function was approximate 644 ksi (4.44 GPa) with a standard deviation of 384 ksi (2.65 GPa). The frequency distributions given by the Monte Carlo Simulation of the different analyses for all the analytical models are shown in Appendix C.

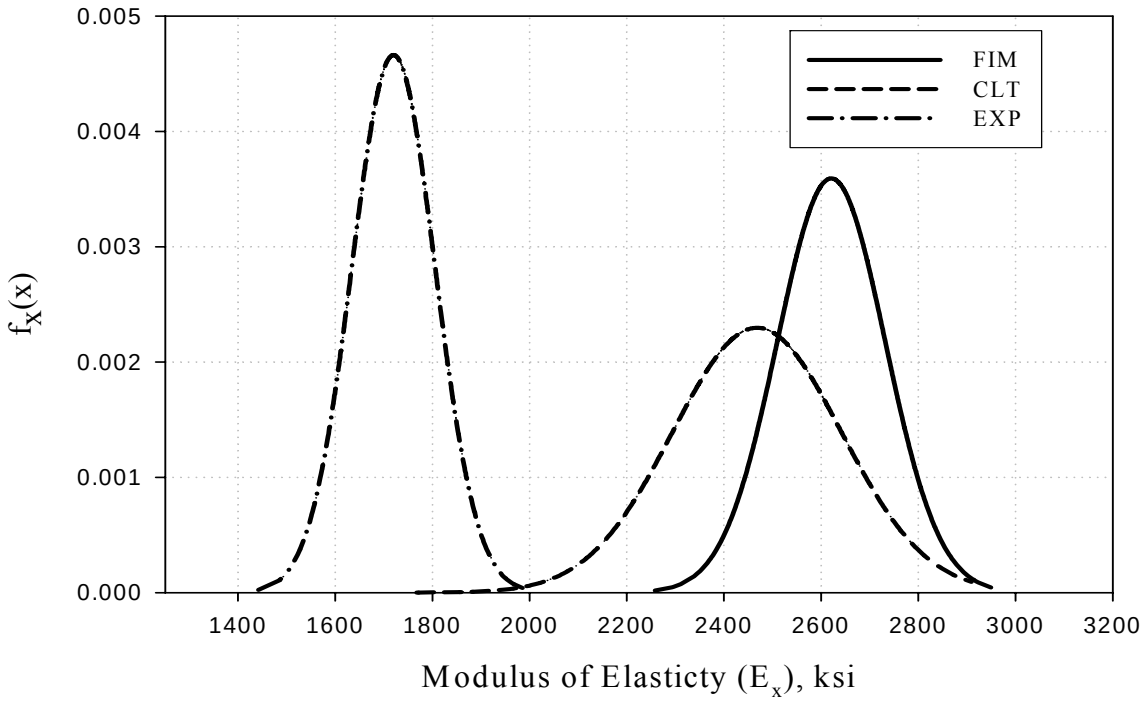

Figure 4.2: Comparison of the Statistical Distribution of the Theoretical Modulus and the Experimental Values in the x-Direction.

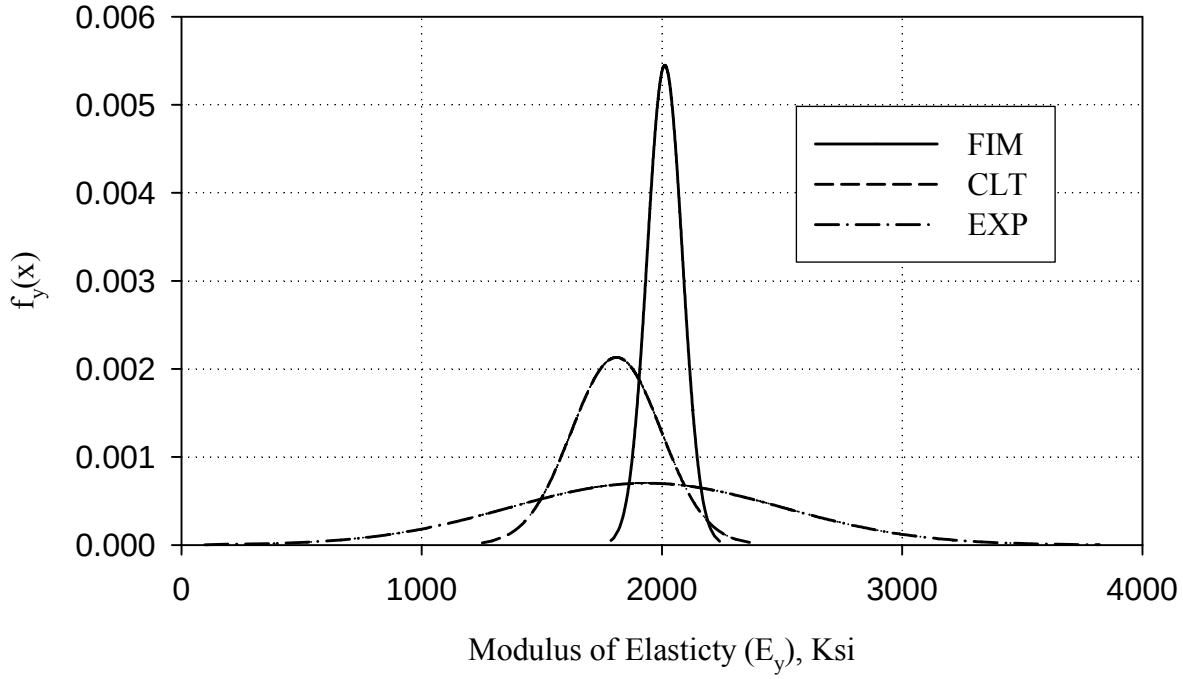

Figure 4.3: Comparison of the Statistical Distribution of the Theoretical Modulus and the Experimental Values in the y-Direction.

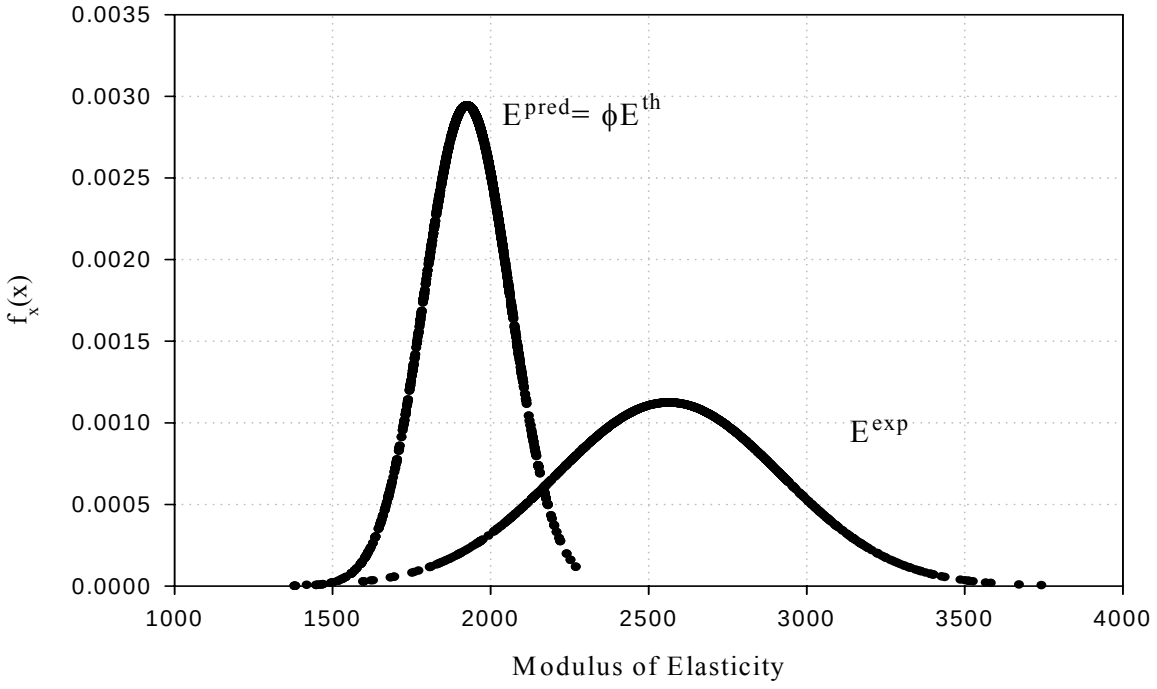

Figure 4.4: Stiffness Reduction Factor ϕ_x (Predicted Design Value), (ϕ_x= 0.59).

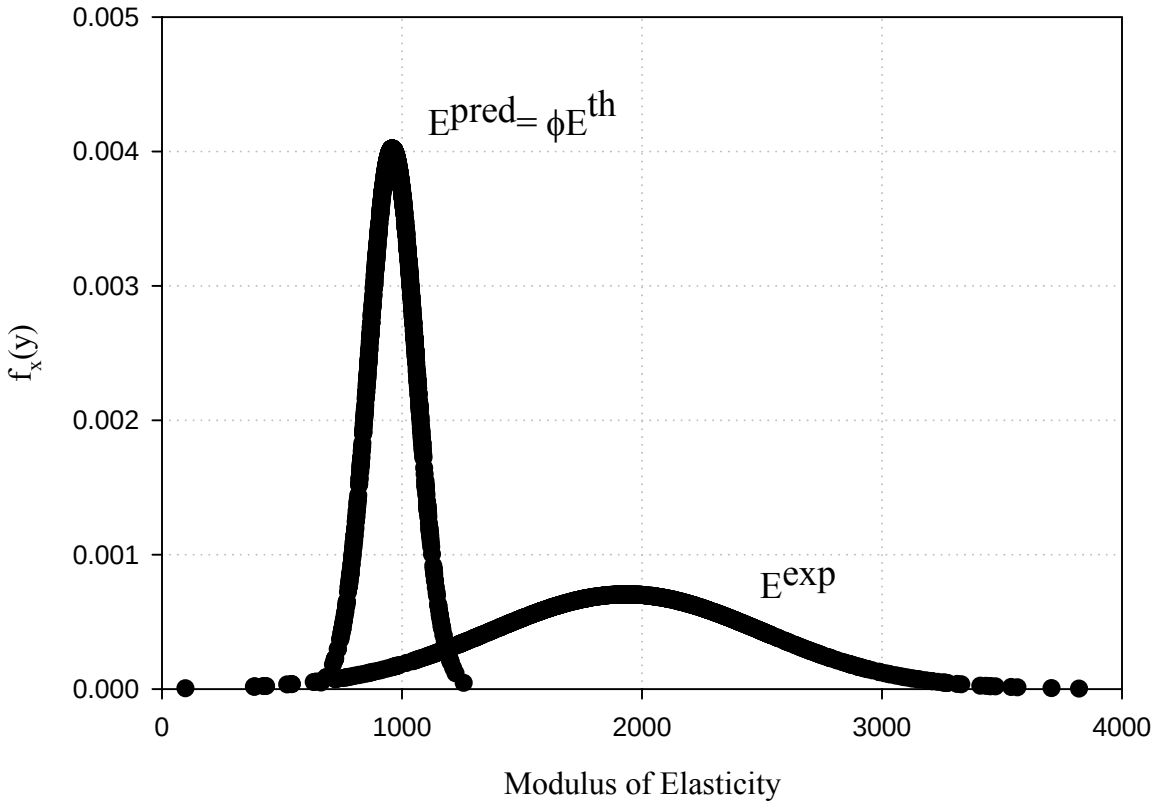

Figure 4.5: Stiffness Reduction Factor ϕ_y (Predicted Design Value), (ϕ_y= 0.76).

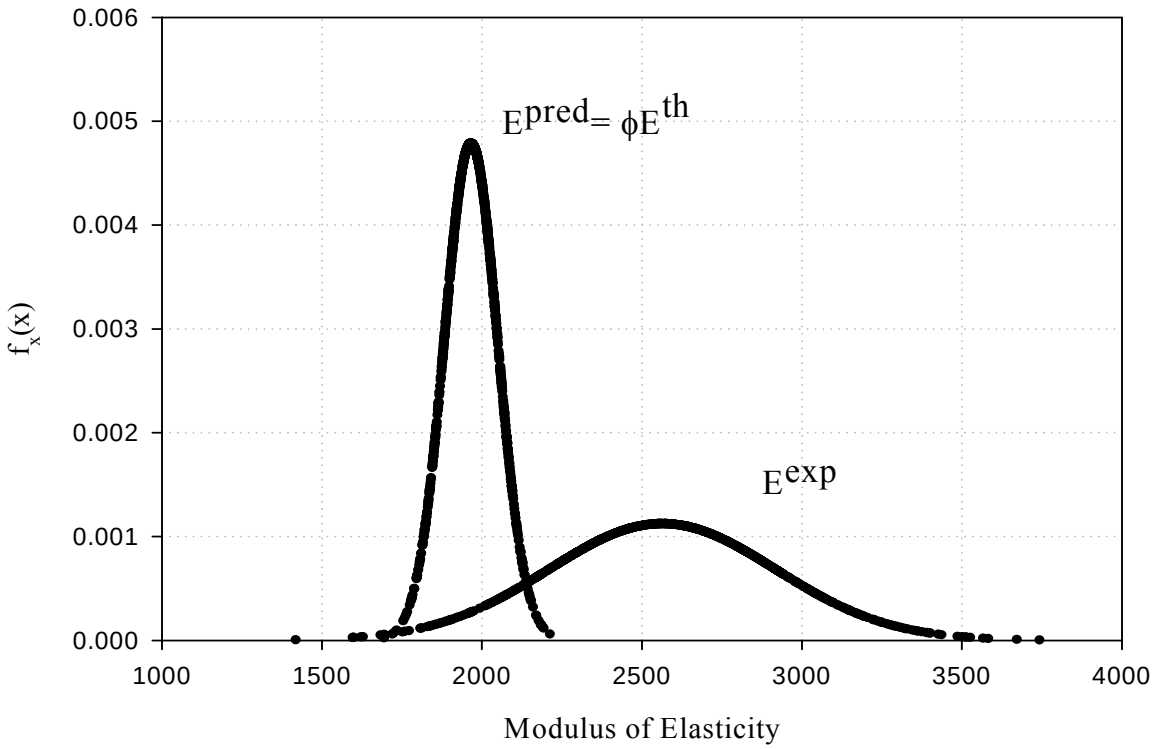

Figure 4.6: Stiffness Reduction Factor ϕ_x (Predicted Design Value), (ϕ_x= 0.53).

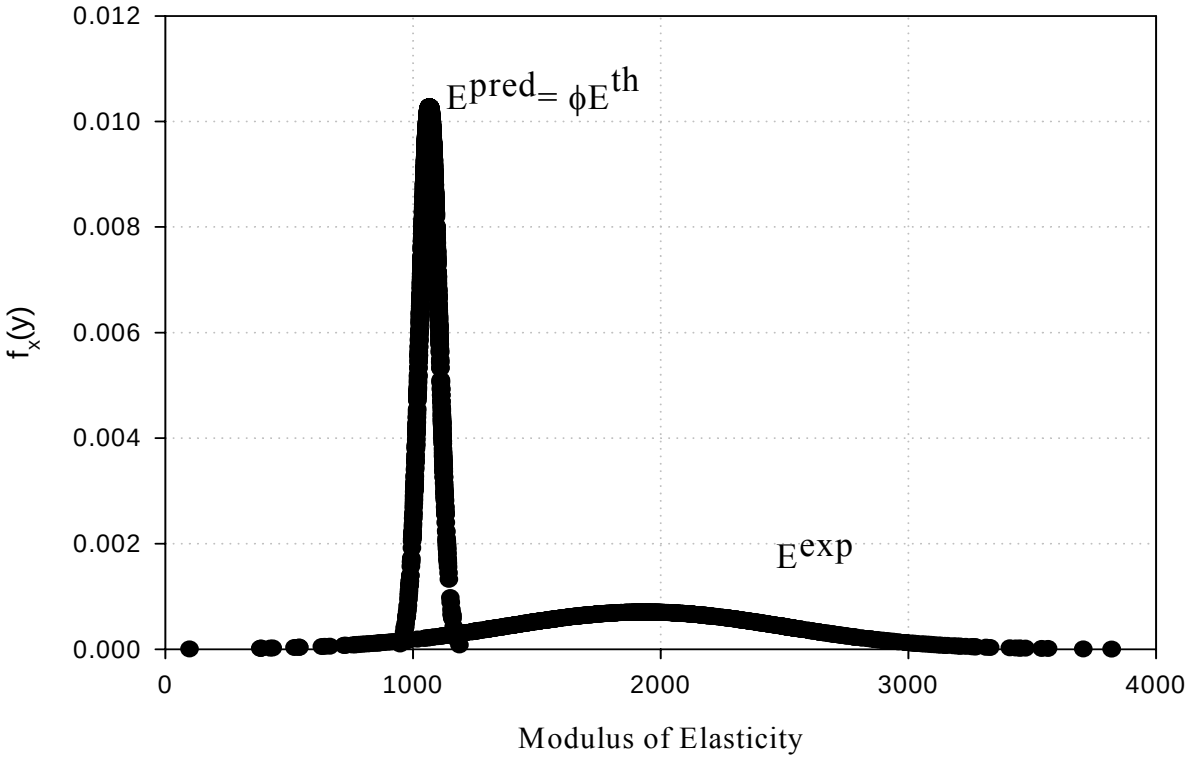

Figure 4.7: Stiffness Reduction Factor ϕ_y (Predicted Design Value), (ϕ_y= 0.75).

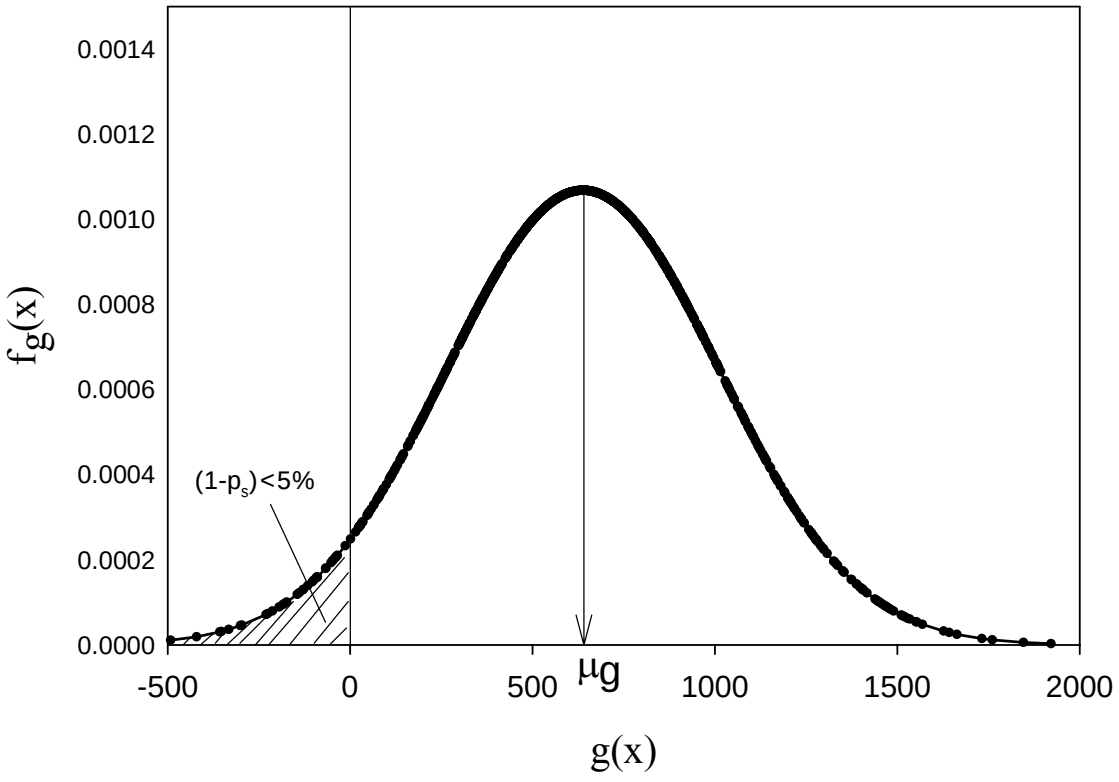

Figure 4.8: Frequency Distribution of Function g(x).

4.4 Analysis of Results

The reduction factors *(ϕ)* that have been evaluated for both, the x and y directions and also compared between two analytical methods (CLT and FIM) are reported in Table 4.3 and Table 4.4, respectively. The tables are divided by their respective directions. From left to right, column 2 has the ϕ factors varying from 0.5 to 1.0. The third and fourth columns have the average and standard deviation respectively. Columns 5 and 6 show results from Equations 4.5 and 4.6 respectively. To estimate a reasonable design ϕ factor, the 95 percentile of the probability was set. Notice that the experimental data with higher variability (x-direction) require smaller ϕ factors than data with lower variability (y-direction). Also these factors are lower for the more precise FIM than for the conservative CLT. This ϕ value complied the condition for the modulus of elasticity to reach the expected value, as mentioned in the previous chapter.

Table 4.3: Variation of the Reduction Factors ϕ Using CLT.

Direction	ϕ	μ_g	σ_g	β	$p_s[g>0]$
x	0.50	462.65	126.65	3.653	99.99
	0.55	337.03	132.84	2.537	99.44
	0.60	207.47	142.43	1.457	92.74
	0.65	85.79	146.97	0.584	72.03
	0.70	-44.03	157.6	-0.279	39.00
	0.75	-165.45	161.86	-1.022	15.33
	0.80	-295.5	173.44	-1.704	4.42
	0.85	-416.69	177.31	-2.350	0.94
	0.90	-597.04	189.8	-3.146	0.08
	0.95	-667.94	193.2	-3.457	0.03
	1.00	-798.5	206.5	-3.867	0.01
y	0.50	1317.67	574.3	2.294	98.91
	0.55	1239.52	579.21	2.140	98.38
	0.60	1196.28	576.57	2.075	98.10
	0.65	1117.8	581.66	1.922	97.27
	0.70	1074.89	579.17	1.856	96.83
	0.75	996.07	584.45	1.704	95.58
	0.80	953.5	582.12	1.638	94.93
	0.85	874.35	587.6	1.488	93.16
	0.90	832.11	585.4	1.421	92.24
	0.95	752.62	591.08	1.273	89.85
	1.00	710.72	589.01	1.207	88.62

Table 4.4: Variation of the Reduction Factors ϕ Using FIM.

Direction	ϕ	μ_g	σ_g	β	$p_s[g>0]$
x	0.5	275.69	114.62	2.405	99.19
	0.55	132.83	121.72	1.091	86.24
	0.60	-12.63	126	-0.100	46.01
	0.65	-155.23	133.69	-1.161	12.28
	0.70	-300.96	138.32	-2.176	1.48
	0.75	-443.3	146.4	-3.028	0.12
	0.80	-589.29	151.26	-3.896	0.00
	0.85	-731.36	159.7	-4.580	0.00
	0.90	-877.62	164.69	-5.329	0.00
	0.95	-1019.43	173.51	-5.875	0.00
	1.00	-1165.95	178.5	-6.532	0.00
y	0.50	1270.24	560.33	2.267	98.83
	0.55	1204.7	552.9	2.179	98.53
	0.60	1141.54	562.34	2.030	97.88
	0.65	1075.62	555	1.938	97.37
	0.70	1012.85	564.69	1.794	96.36
	0.75	946.53	557.44	1.698	95.52
	0.80	884.16	567.38	1.558	94.04
	0.85	817.44	560.21	1.459	92.77
	0.90	755.46	570.4	1.324	90.73
	0.95	688.36	563.32	1.222	88.91
	1.00	626.77	573.75	1.092	86.27

The final proposed ϕ factor was determined by linear interpolation between the values of which the 95% of p_s appears. Figure 4.9 shows the variation of the function $p_s[g>0]$ vs. the ϕ factors. In this figure it can be seen that the ϕ factors that make the $p_s>95\%$ (Equation4.6) are lower and upper bound between both methods. The difference between the ϕ factors in the x-direction by both analytical methods, CLT and FIM, which the values were ϕ_x= 0.59 and ϕ_x= 0.53 respectively, is 0.06, otherwise in the y-direction with the same methods, the difference between ϕ_y = 0.75 and ϕ_y =0.76 is 0.01. The differences between the models represent the precision in the analysis between both methods and how close they are to the experimental value. Comparing this reduction factor values with the conclusions of Zureick and Steffen (2000) which is 0.50 for compressive failure, and Acosta (1999), which is 0.55 for tensile load, it could be conclude that there exists an acceptable relation between them. Acosta (1999) performed the analysis with the same material (FRP) with less number of samples and performed the analysis only with the CLT model.

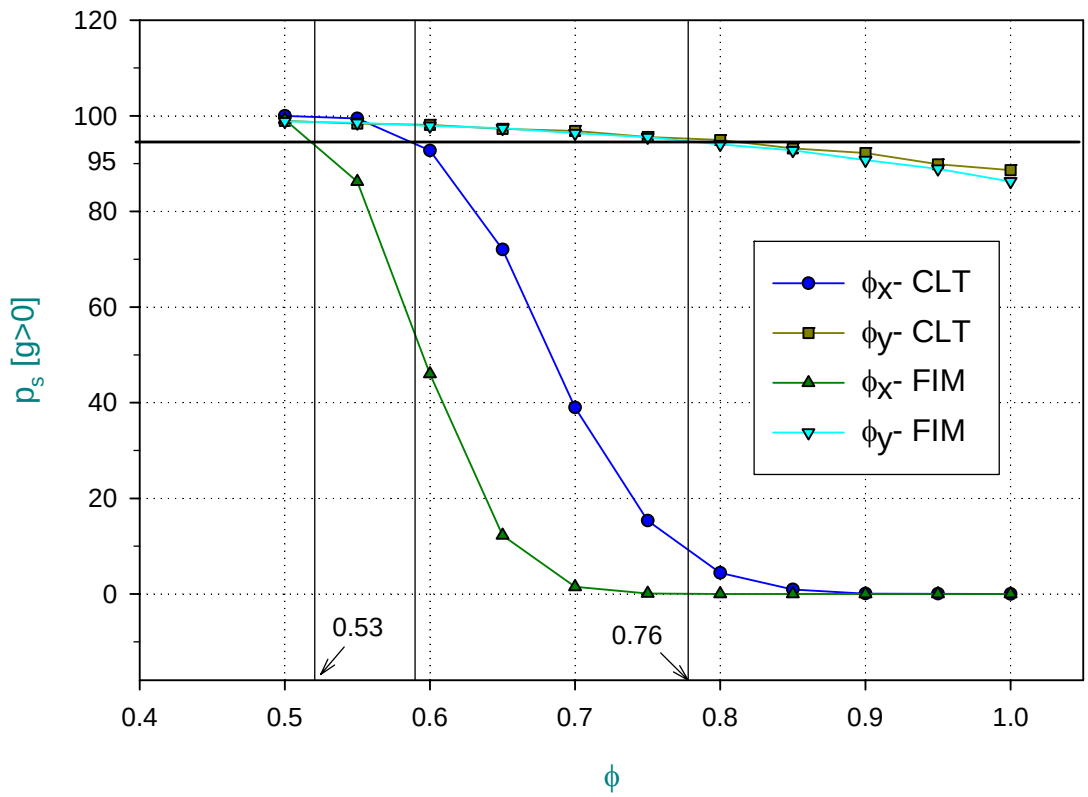

Figure 4.9: Variation of the Probability vs. ϕ Factor.

4.5 Parametric Analysis

The mechanical properties of the material have been evaluated with different models and specific properties. An analysis of the material varying the principal mechanical properties *(E_f and E_m)* was performed to evaluate its effect in the reliability model. For the analysis, the modulus remained constant but the standard deviations were changed according to CV of 5%, 10%, and 15%. Another analysis that was performed is the evaluation of the material modulus of elasticity with variations in manufacturing properties. These properties are the fiber volume fraction *(v_f)* and the braid orientation angle *(θ_b)* of the FRP. Figure 4.10 shows a chart of the elastic modulus with variation of θ, E_m and E_f with respect to changes in *CV*. It can be seen in Figure 4.10 that the modulus of elasticity was not considerably affected by changes in the constituent's modulus. However, a notable difference is observed from changes in the fiber orientation. The results are presented in Figure 4.11, 4.12 and 4.13 for the different directions and models.

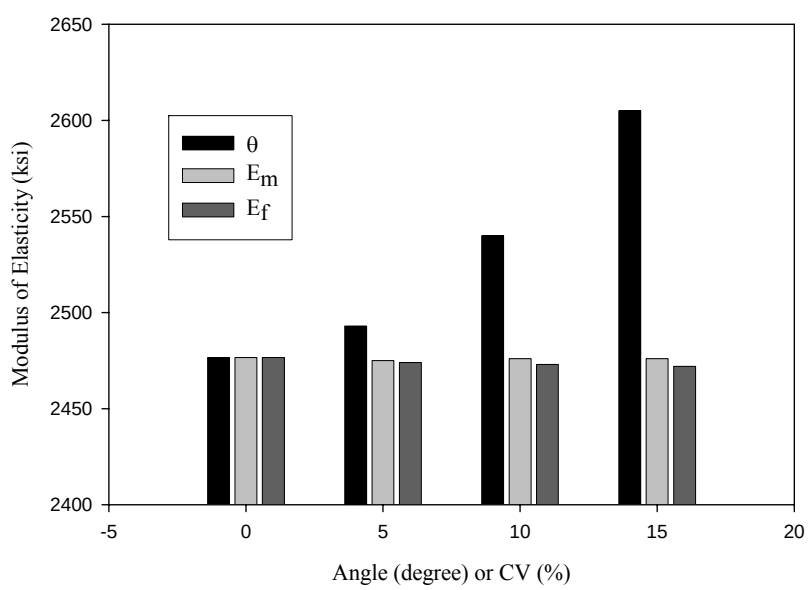

Figure 4.10: Parametric Analysis of the Different Material Properties- Classical Lamination Theory- E_x.

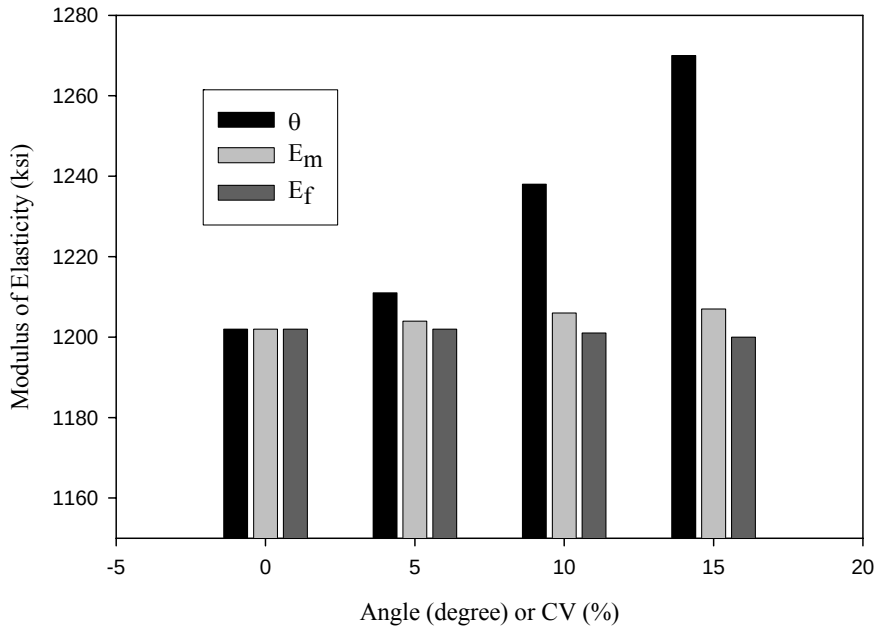

Figure 4.11: Parametric Analysis of the Different Material Properties- Classical Lamination Theory- E_y.

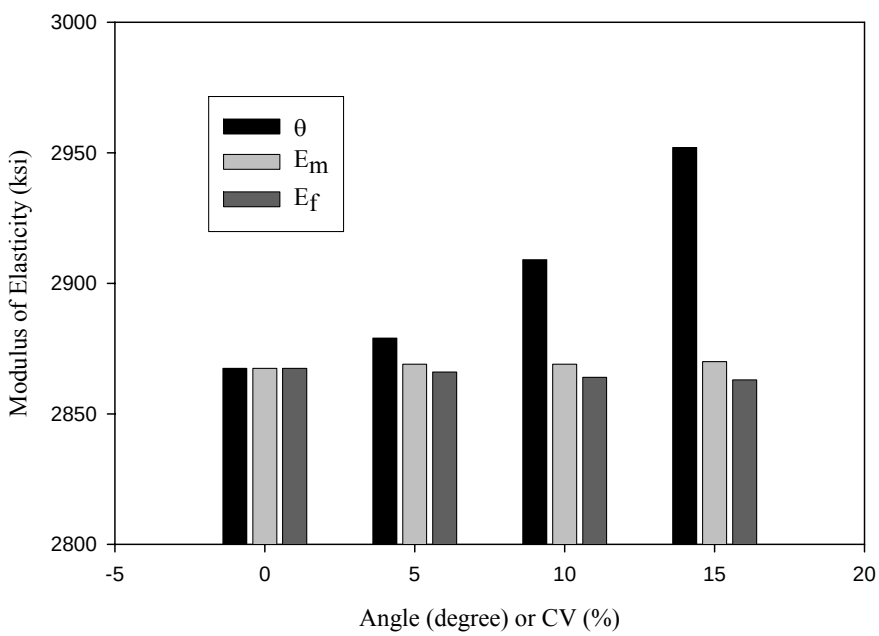

Figure 4.12: Parametric Analysis of the Different Material Properties- Fiber Inclination Model- E_x.

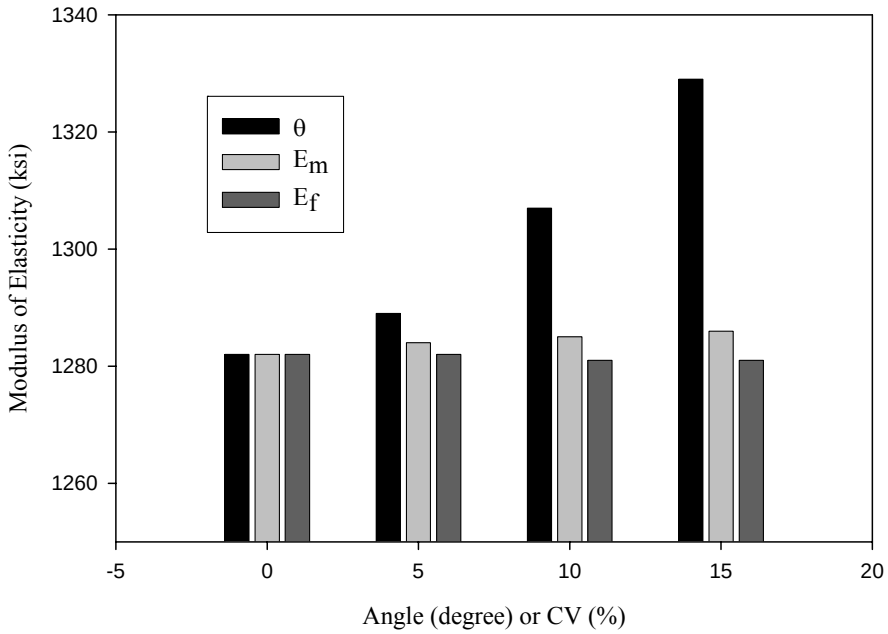

Figure 4.13: Parametric Analysis of the Different Material Properties- Fiber Inclination Model- E_y.

From this study it is concluded that the orientation of the fiber is the most sensitive parameter that generate considerable differences in the moduli values. The orientation of the fiber creates a notable difference of 2.60% between the different conditions. These variations are reported in Appendix D. Otherwise, the other properties (E_m and E_f) just generate a difference of 0.078%. This difference is so small compared to the angle that it is reasonable to ignore it. This analysis with the three properties mentioned can define that the orientation of the fiber is a variable that control the design of the material.

Another variable that was studied is the fiber volume fraction (v_f). The variation related to the fiber volume fraction was performed varying its value from 0.25 to 0.65 combined with variation of the mechanical properties. These variations are also reported in Appendix E. The results of the study are plotted in Figure 4.14 and 4.15 for the CLT in the x and y-direction respectively, and in Figures 4.16 and 4.17 for the FIM model in the x and y-direction respectively.

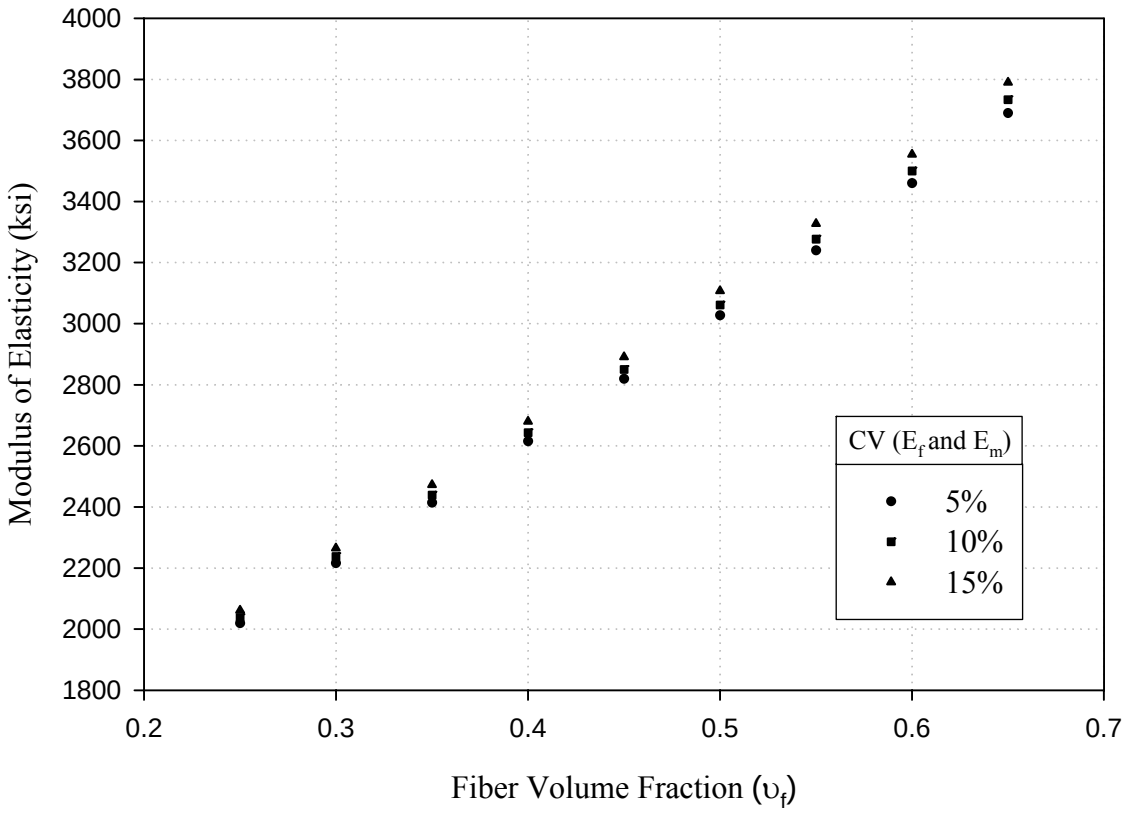

Figure 4.14: Modulus of Elasticity with Variation in Fiber Volume Fraction Classical Lamination Theory- E_x .

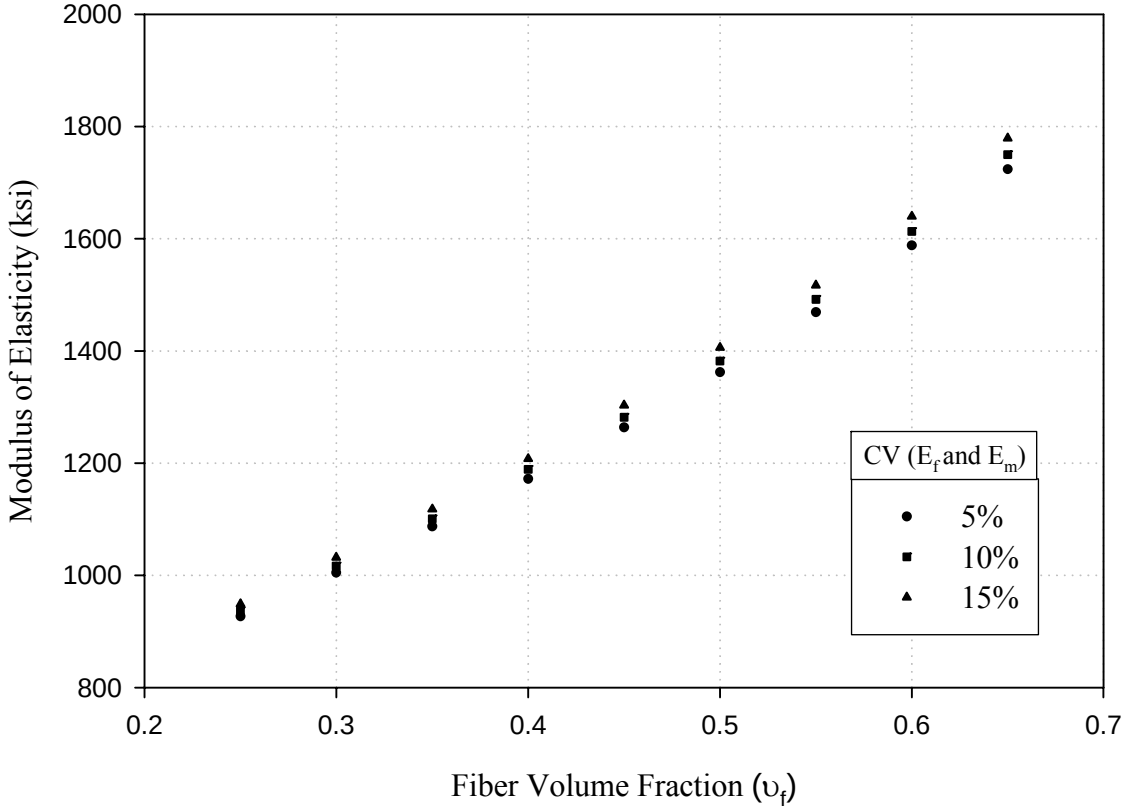

Figure 4.15: Modulus of Elasticity with Variation in Fiber Volume Fraction Classical Lamination Theory- E_y.

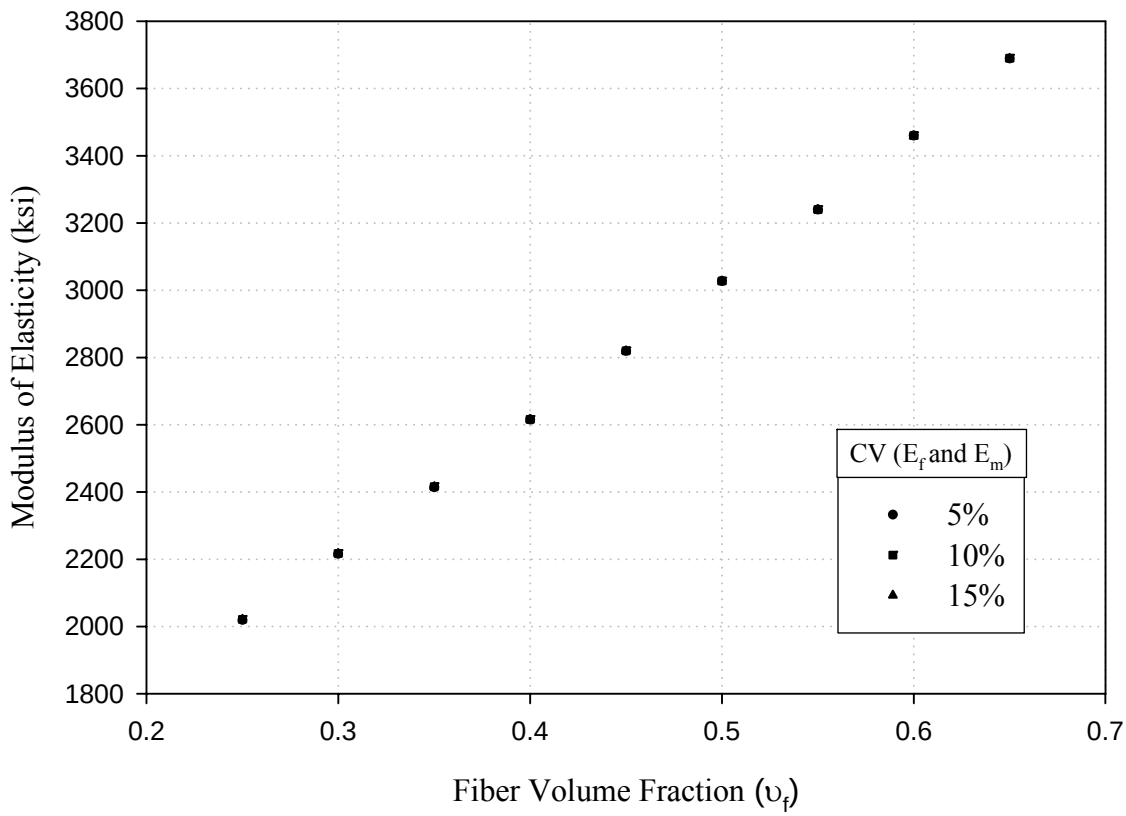

Figure 4.16: Modulus of Elasticity with Variation in Fiber Volume Fraction Fiber Inclination Model- E_x.

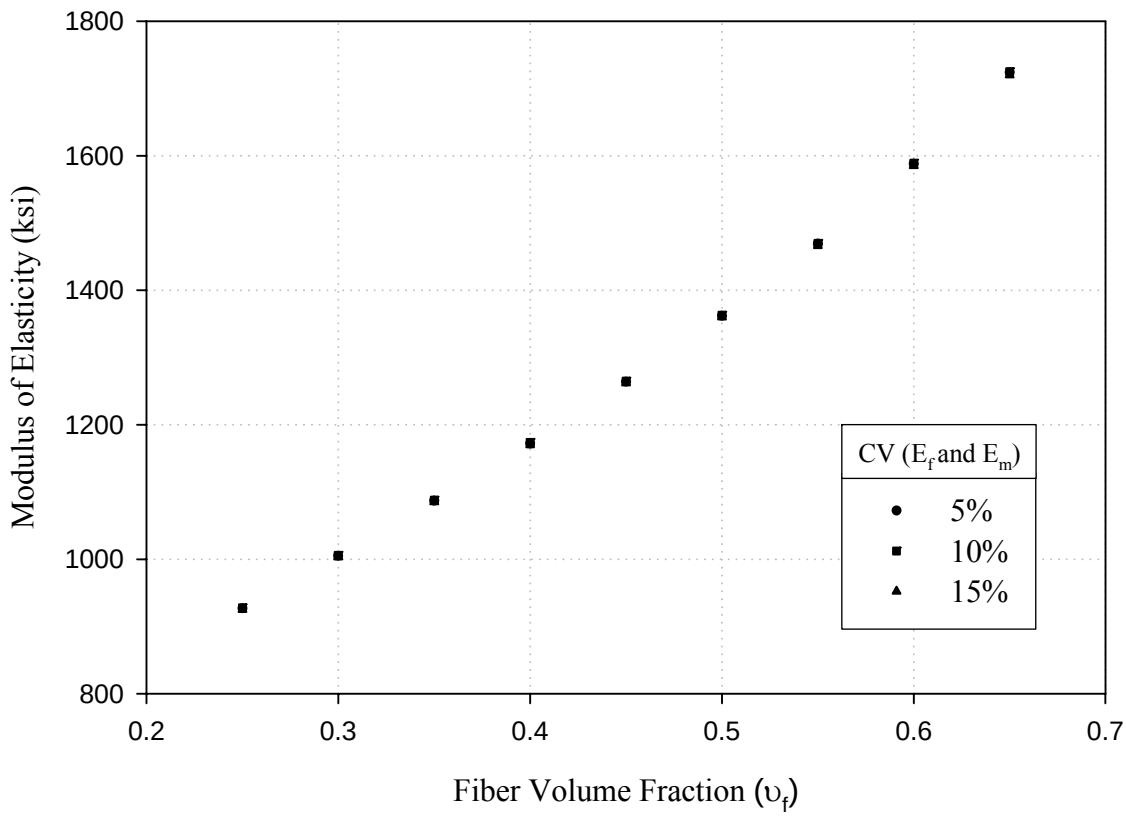

Figure 4.17: Modulus of Elasticity with Variation in Fiber Volume Fraction Fiber Inclination Model- E_y.

As it is seen in the figures, the variations of the fiber volume fraction affects the modulus of elasticity directly, but not the variations of the mechanical properties of the matrix and fibers. Also it can be seen that the variation of the properties do not affect the values of the reduction ϕ factor. Figures 4.18 and 4.19 show graphs similar to the ones in Figures 4.9 but incorporating the 10% and 15% *CV* for the constituents properties. In Figure 4.18, the ϕ factors are 0.48 and 0.75 in the x-direction and the y-direction, respectively, for the 10% CV. Similarly, from Figure 4.19 it is found ϕ factors of 0.48 and 0.75 in the x-direction and the y-direction, respectively, for the 15% properties variation. Comparing these values with the values determined in the original analysis (5% property variation, Figure 4.5*)*, the difference are 2.47% for both methods in the x-direction, and 0.33% for both methods in the y-direction respectively. It is concluded that the reduction factors ϕ are not affected by the variation of the mechanical properties of the constituents. However change in fiber volume fraction affect significantly the modulus of the material.

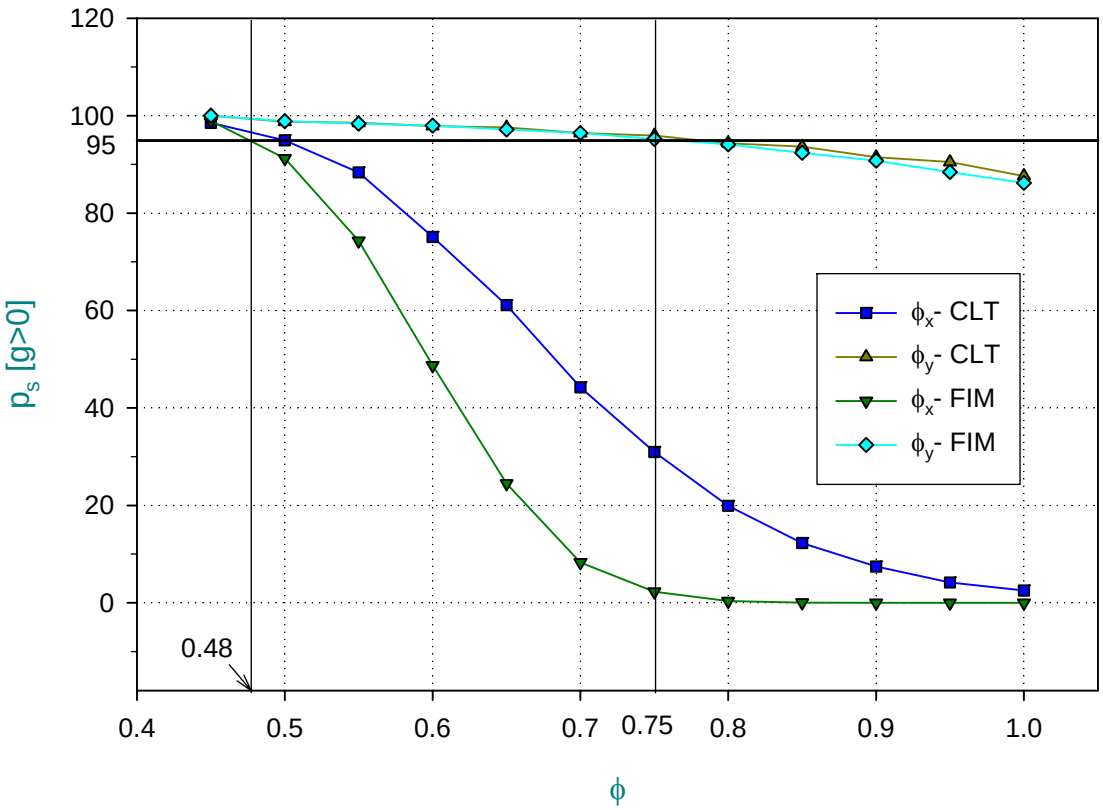

Figure 4.18: Variation of the Probability vs. ϕ Factor - 10% Standard Deviation.

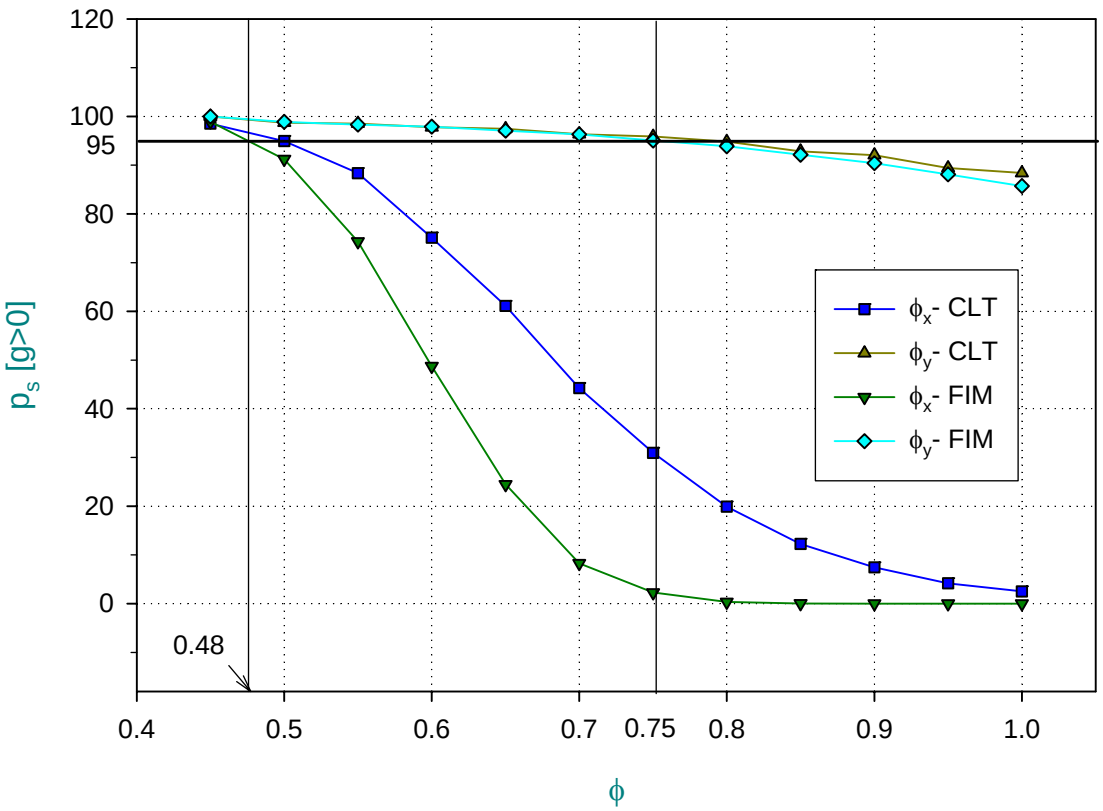

Figure 4.19: Variation of the Probability vs. ϕ Factor - 15% Standard Deviation.

4.6 Proposed Reduction Factors

After performing all the reliability analyses in both principal directions using two theoretical formulations for the FRP, a reduction factors ϕ for the material moduli are suggested. Considering that the differences between the moduli reduction factors are minimal, to be conservative, the recommended reduction ϕ factor will be the smallest of both values of the principal directions, since it will control the design. Table 4.5 reports the two values recommended and at this point two separate values are proposed, one for each material direction

Table 4.5: Capacity Reduction Factor.

Direction of the Fiber	**ϕ**
x- Direction	0.50
y- Direction	0.75

To address the effectiveness of the proposed factors, the $E^{exp}/\phi E^{th}$ ratios for each data values were computed. Results are reported in Figures 4.20 and 4.21 for CLT and Figures 4.22 and 4.23 for FIM. From the figures it is observed that the ϕ factors had effectively provided a confidence in the results, having only a few data samples below a ratio of 1. The values below 1 represent the 5% risk allowed in the formulation.

From the figures it could be concluded that the proposed reduction factors ϕ= 0.50 fulfill the requirement that the experimental modulus of elasticity values for the FRP exceed the values estimated from the analytical models.

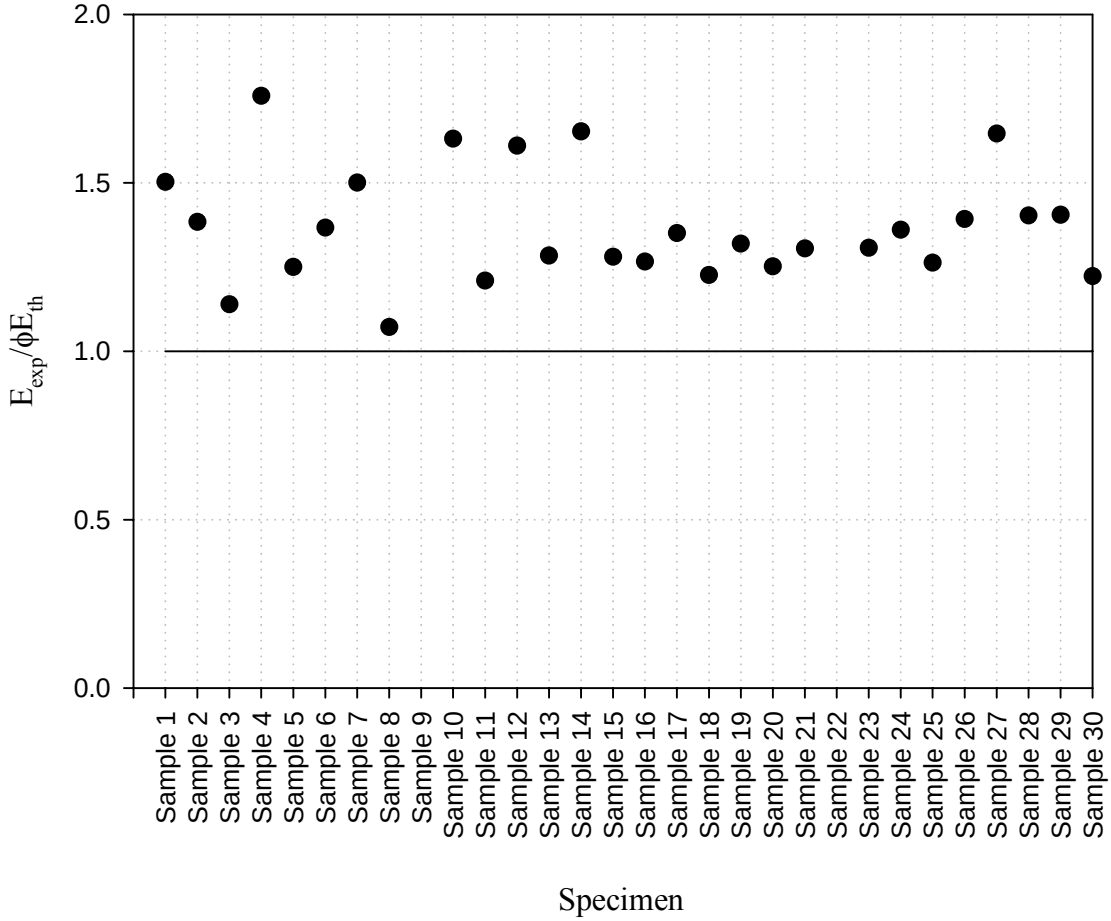

Figure 4.20: Experimental vs. Predicted Modulus of Elasticity for all the Coupons Tested in the Longitudinal Direction using CLT.

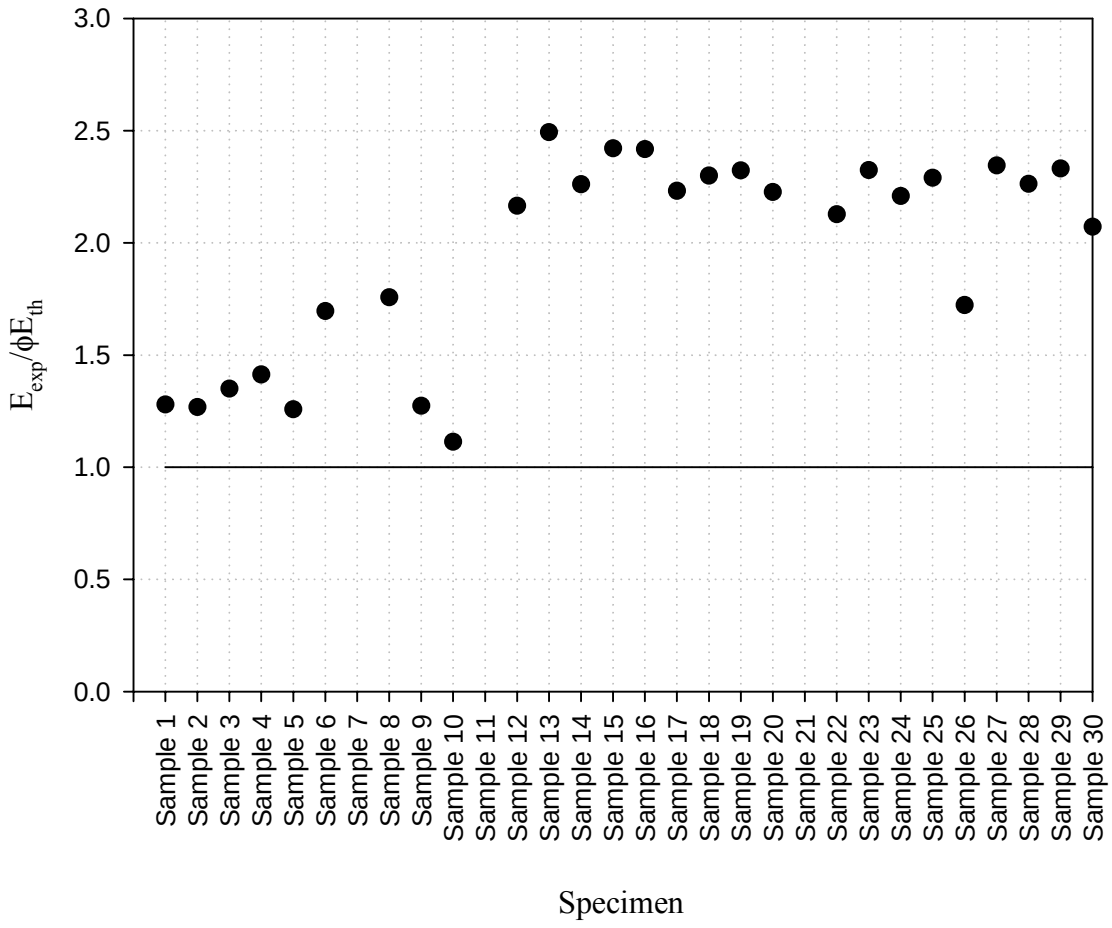

Figure 4.21: Experimental vs. Predicted Modulus of Elasticity for all the Coupons Tested in the Transverse Direction using CLT.

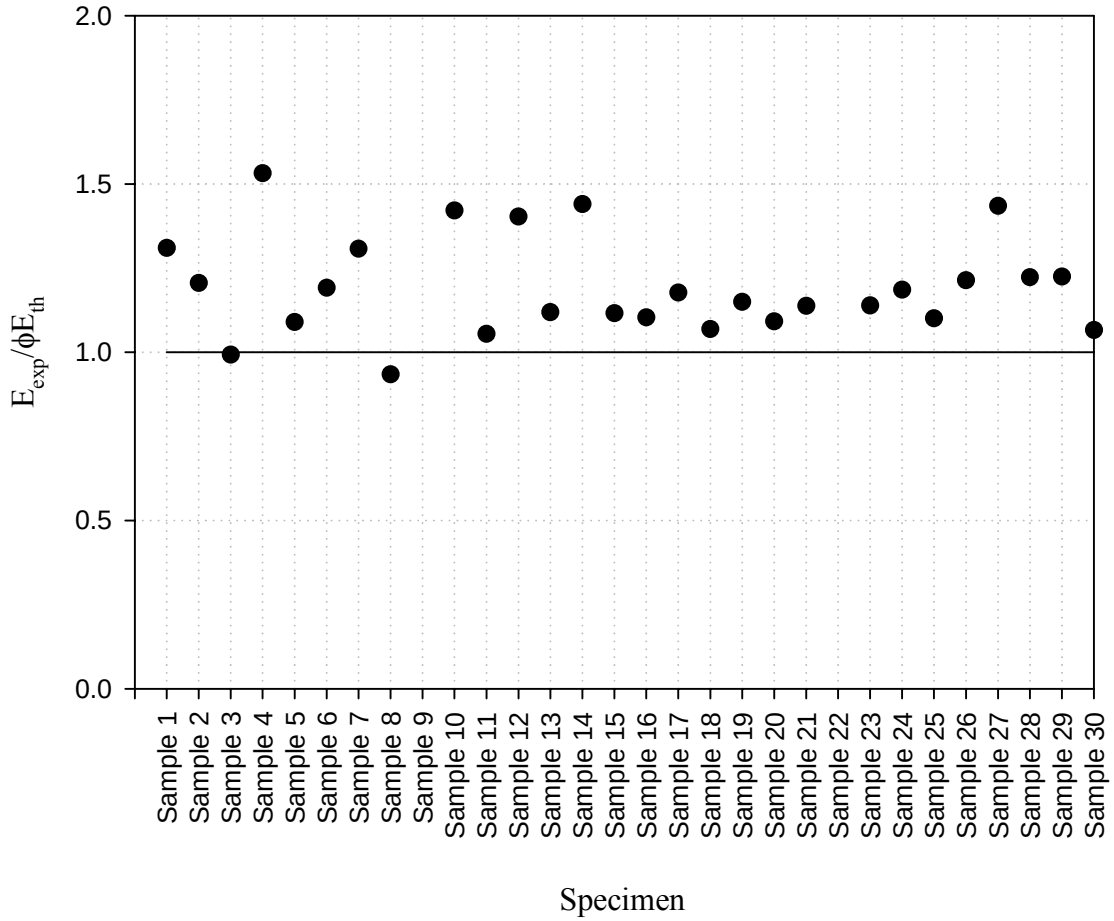

Figure 4.22: Experimental vs. Predicted Modulus of Elasticity for all the Coupons Tested in the Longitudinal Direction using FIM.

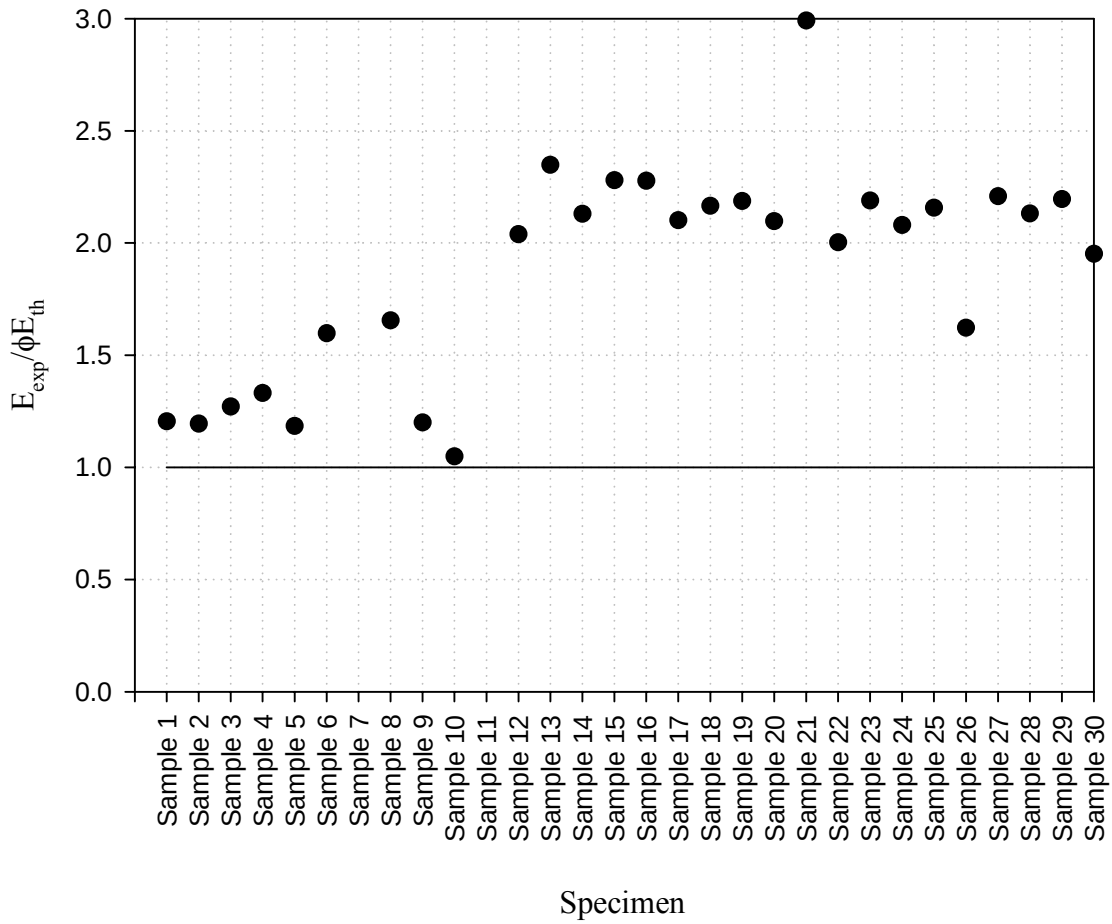

Figure 4.23: Experimental vs. Predicted Modulus of Elasticity for all the Coupons Tested in the Transverse Direction using FIM.

CHAPTER V
CONCLUSIONS AND RECOMMENDATIONS

5.1 Introduction

This Chapter presents the conclusions of the research and recommendations of the author based on the fulfillment of the main objectives.

5.2 Project Summary

The Fiber-Reinforced Polymer (FRP) studied in the project is a vinyl ester resin reinforced with E-glass fibers in the form of a three- dimensional braided textile. As part of the objectives of the project, the characterization of the FRP was performed in tensile tests with the material orientation in the principal longitudinal and transverse directions. The modulus of elasticity was measured according with the *ASTM D 3039* standard. The *ASTM* indicates that the modulus of elasticity should be determined by the chord method, but due to the variation of the material behavior during the test, the moduli were calculated by linear regression. Also different methods have been used to estimate the modulus of elasticity of the material.

To estimate the theoretical value of the modulus of elasticity, two analytical models were considered. These models were Classical Lamination Theory (CLT) and the Fiber Inclination Model (FIM). To consider the variability in the constituent's mechanical properties (modulus of elasticity of the fiber and the matrix) of the FRP, the models assumed a 5% variation in these properties maintaining the mean value constant. This variability was simulated by the Monte Carlo Simulation technique. The Monte Carlo Simulation generates randomized values approximating the properties of the material to

estimate the characteristic value. The experimental data were reduced using statistical analysis and compared with results of the analytical models. Analyzing the differences between the experimental values with each analytical method multiplied by a reduction ϕ factor (Performance Function), the probability to be more than cero was determined. The reduction factor for the design of the material is determined by the factor that made this probability grater than 95%. The ϕ factor was determined for both directions, x and y-directions. This reduction ϕ factor is proposed to be used to determinate the desired design modulus of elasticity for similar FRP´s.

5.3 Conclusions

After performing the reliability-based analysis of the pultruded FRP reinforced with 3D braid, the following conclusions are drawn:

- Although the FIM accounts for the 3D structure of the braid, in general, both models do not give an accurate representation of the material properties. However, both models gave reasonable results along the transverse (y) directions. Roving was unevenly spaced in the x-direction causing variability. The material was more uniform in the y-direction.
- The reduction factors variability could be explained by the variability of the mechanical properties used in the analytical models.
- The proposed reduction ϕ factors for the stiffness design of the pultruded material reinforcement with a 3D braided textile are ϕ_x= 0.50 and ϕ_y= 0.75.

- The parametric analysis indicated that the fiber orientation and the fiber volume fraction are the variables that mostly control the variability of the material. Variation of the mechanical properties of the constituents has very little effect.

5.4 Recommendations

- Expand the study knowing precisely the variation in the constituents mechanical properties.
- Develop finite element analyses at the micromechanical level of the material to estimate the stress distribution along the different constituents of the composite.
- Because it was found that the fiber content is one of the sensitive variables in the models, this property should be determinate from random peaces to have a more realistic statistical variability.

REFERENCES

- Acosta, F.J. and Roman, J.A. (2004). “Probabilistic Assessment of the Mechanical Properties of a 3D-Braided Pultruded Fiber-Reinforced Polymer”, *International Latin American and Caribbean Conference for Engineering and Technology (LACCEI),* Miami, FL.
- Acosta, F.J. (2002). "Reliability-Based Reduction Factors for Fiber-Reinforced Polymers", *Development in theoretical and Applied Mechanics,* Kassab, Nicholson, and Ionescu Eds.,Vol. 21, Rivercross Publishing, Inc., Orlando, Fl., pp. 335-342.
- Acosta-Costa, F. J. (1999). *Mechanical Characterization of the Mechanical and Structural Properties of Fiber Reinforced Polymeric Bridge Deck Components*, Ph.D. Thesis, Georgia Institute of Technology, Atlanta, GA. , 394 pages.
- ASTM D 3039, “Standard Test Method for Tensile Properties of Polymer Matrix Composite Materials”, ASTM International.
- Azzi, V.D. and Tsai, S.W. (1964). “Elastic Moduli of Laminate Anisotropic Composite,” *SESA Annual Meeting,* Cleveland Ohio.
- Barbero, E.J. (1998). *Introduction to Composite Materials Design*, Taylor and Francis, pp. 68-72.
- Brown, R. T., and Crow, E. C. (1992). “Automatic Through-the-Thickness Braiding,” *37th International SAMPE Symposium*, pp. 832-842
- Ceroni, F., Pecce, M., and Matthys, S. (2004). “Tension Stiffening of Reinforced Concrete Ties Strengthened with Externally Bonded Fiber-Reinforced Polymer Sheets”, *Journal of Composite Material for Constructions,* Vol. 8, No.1, pp.22-32.

- Chou, T. (1992). *Microstructural design of fiber composite*, Cambridge University Press, New York.
- Harr, M. E., (1987) *Reliability-Based Design in Civil Engineering*. Dover Publications, Inc., Mineola, NY.
- Decisioneering, Inc. (2000). <http://www.decisioneering.com/monte-carlo-simulation.html> (2003)
- Deitz, D.H., Harik, I.E., and Gesund, H. (2003). "Physical Properties of Glass Fiber Reinforced Polymer Rebars in Composite", *Journal of Composite Material for Constructions*, Vol. 7, No. 4 , pp. 363-366.
- Lundberg, J.E. and Galambos, T.V. (1996). "Load and Resistance factor design of composite columns", *Structural Safety,* Vol.18, No.2, pp. 169-177.
- Val, D.V. (2003). "Reliability of Fiber- Reinforced Polymer- Confined Reinforced Concrete Columns", *Journal of Composite Material for Constructions*, Vol. 129, No. 8, pp. 1122-1130.
- Williams, B., Shehata, E., and Rizkalla, S. H. (2003). "Filament-Wound Glass Fiber reinforced Polymer Bridges Deck Modules", *Journal of Composite Material for Constructions,* Vol. 7, No.3, pp. 266-273.
- Yeh, H.L. and Yeh, H.Y. (2000). "Elastic moduli of laminate composite revised by using statistical analysis", *Composites: Part B, Vol. 31*, pp. 57-64.
- Zureick A. and Steffen R. (2000). "Behavior and Design of Concentrically Loaded Pultruded Angle Struts", *Journal of Structural Engineering,* Vol.126, No.3, pp.406-416.

APPENDIX A

A.1: Samples Dimensions and Experimental Results for Longitudinal Direction.

Sample	Width	Thickness	Area	Load	Strength
1	2.0748	0.2322	0.4817	7.80	16.19
2	2.0788	0.2325	0.4833	7.92	16.39
3	2.0660	0.2345	0.4845	8.99	18.55
4	2.0733	0.2328	0.4827	9.74	20.18
5	2.0727	0.2325	0.4819	9.74	20.21
6	2.0583	0.2327	0.4789	8.48	17.71
7	2.0598	0.2370	0.4882	7.66	15.69
8	2.0792	0.2350	0.4886	3.03	6.21
9	2.0723	0.2340	0.4849	9.66	19.92
10	2.0605	0.2135	0.4399	9.87	22.44
11	2.0637	0.2343	0.4836	6.59	13.64
12	2.0527	0.2077	0.4263	9.85	23.10
13	2.0620	0.2322	0.4787	6.99	14.60
14	2.0627	0.2387	0.4923	8.47	17.21
15	2.0602	0.2370	0.4883	6.80	13.92
16	2.0557	0.2150	0.4420	5.91	13.36
17	2.0590	0.2350	0.4839	7.72	15.96
18	2.0623	0.2218	0.4575	8.26	18.05
19	2.0598	0.2363	0.4868	8.64	17.75
20	2.0625	0.2073	0.4276	5.71	13.35
21	2.0618	0.2078	0.4285	6.27	14.64
22	2.0628	0.2342	0.4830	9.49	19.65
23	2.0613	0.2082	0.4291	6.98	16.25
24	2.0600	0.2292	0.4721	6.64	14.07
25	2.0642	0.2082	0.4297	5.42	12.62
26	2.0635	0.2085	0.4302	6.99	16.25
27	2.0582	0.2388	0.4916	7.93	16.14
28	2.0630	0.2070	0.4270	8.05	18.85
29	2.0602	0.2107	0.4340	8.54	19.68
30	2.0622	0.2083	0.4296	8.28	19.26
Average	2.0638	0.2248	0.4639	7.75	16.73
Stdev	0.0065	0.0124	0.0261	1.56	3.37
C.V.	0.31	5.53	5.63	20.17	20.15

A.2: Samples Dimensions and Experimental Results for Transverse Direction.

Sample	Width	Thickness	Area	Load	Strength
1	1.2652	0.2397	0.3032	1.95	6.45
2	1.2597	0.2403	0.3027	2.14	7.07
3	1.2520	0.2413	0.3021	2.30	7.62
4	1.2575	0.2373	0.2984	2.60	8.70
5	1.2538	0.2410	0.3022	2.51	8.30
6	1.2482	0.2378	0.2969	3.43	11.55
7	1.2367	0.2370	0.2931	2.14	7.29
8	1.2450	0.2403	0.2992	3.86	12.91
9	1.2498	0.2397	0.2995	2.27	7.56
10	1.2543	0.2383	0.2989	1.91	6.40
11	1.2777	0.2360	0.3015	4.26	14.14
12	1.2823	0.2377	0.3048	4.51	14.80
13	1.2833	0.2377	0.3050	4.72	15.47
14	1.2832	0.2390	0.3067	4.83	15.74
15	1.2827	0.2393	0.3070	4.82	15.70
16	1.2827	0.2353	0.3019	3.54	11.73
17	1.2840	0.2357	0.3026	4.61	15.23
18	1.2807	0.2393	0.3065	4.83	15.76
19	1.2833	0.2380	0.3054	4.79	15.70
20	1.2800	0.2367	0.3029	4.82	15.91
21	1.2800	0.2360	0.3021	4.61	15.27
22	1.2838	0.2365	0.3036	4.07	13.42
23	1.2880	0.2347	0.3023	4.25	14.05
24	1.2827	0.2357	0.3023	4.47	14.78
25	1.2825	0.2343	0.3005	3.85	12.80
26	1.2743	0.2383	0.3037	3.27	10.78
27	1.2760	0.2377	0.3033	3.40	11.22
28	1.2827	0.2350	0.3014	4.15	13.77
29	1.2803	0.2373	0.3039	4.55	14.98
30	1.2813	0.2367	0.3032	4.30	14.18
Average	1.2718	0.2377	0.3022	3.73	12.31
Stdev	0.0150	0.0019	0.0030	1.02	3.32
C.V.	1.18	0.80	0.98	27.49	26.99

APPENDIX B

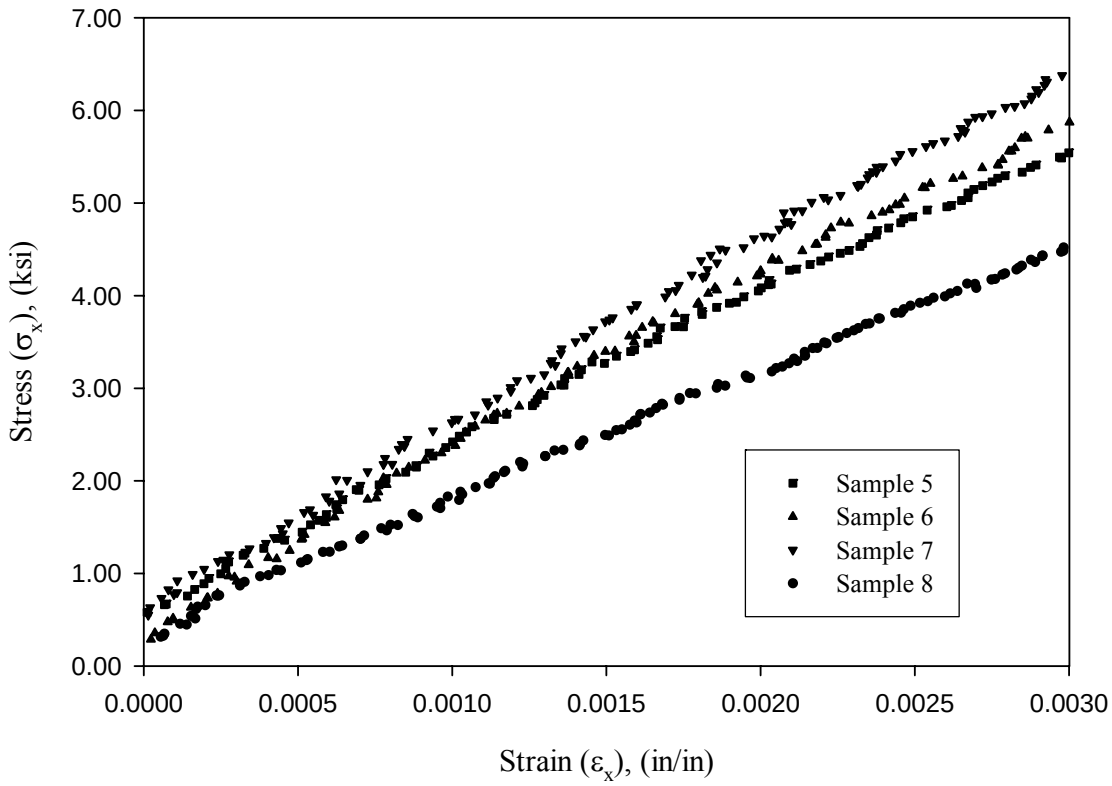

B.1: Initial Portion of a Typical Stress- Strain Curve for Coupons in the Longitudinal Direction.

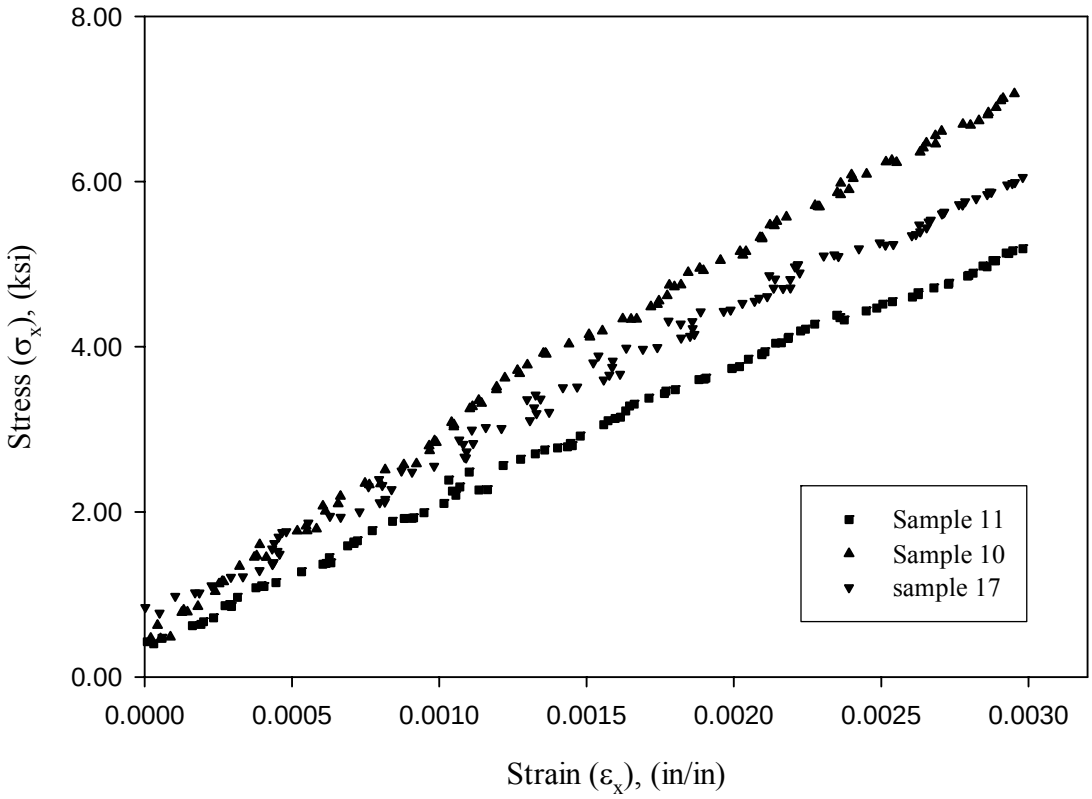

B.2: Initial Portion of a Typical Stress- Strain Curve for Coupons in the Longitudinal Direction.

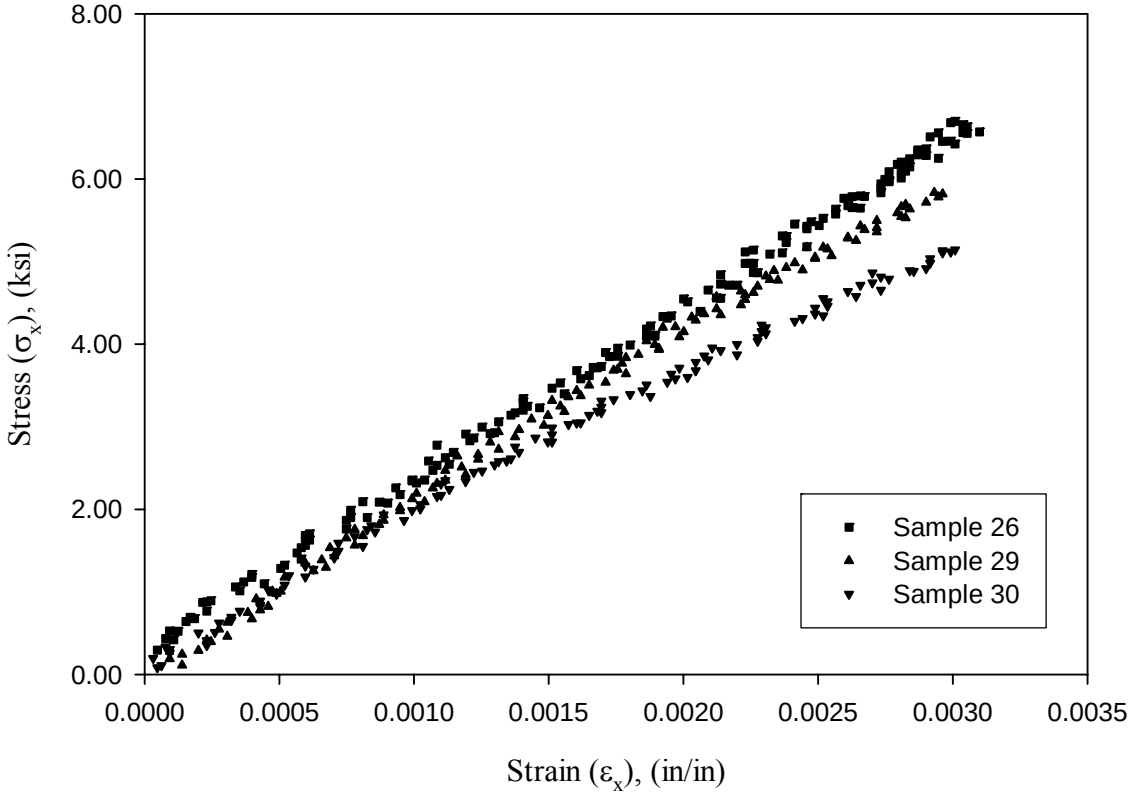

B.3: Initial Portion of a Typical Stress- Strain Curve for Coupons in the Longitudinal Direction.

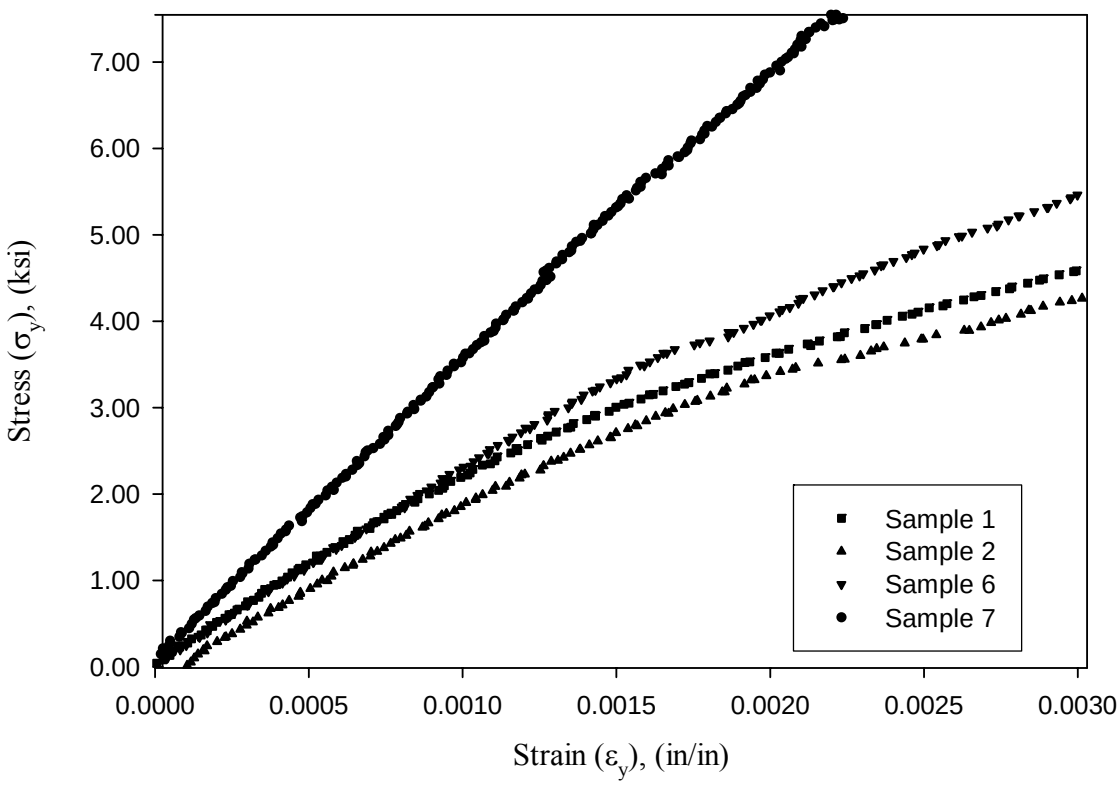

B.4: Initial Portion of a Typical Stress- Strain Curve for Coupons in the Transverse Direction.

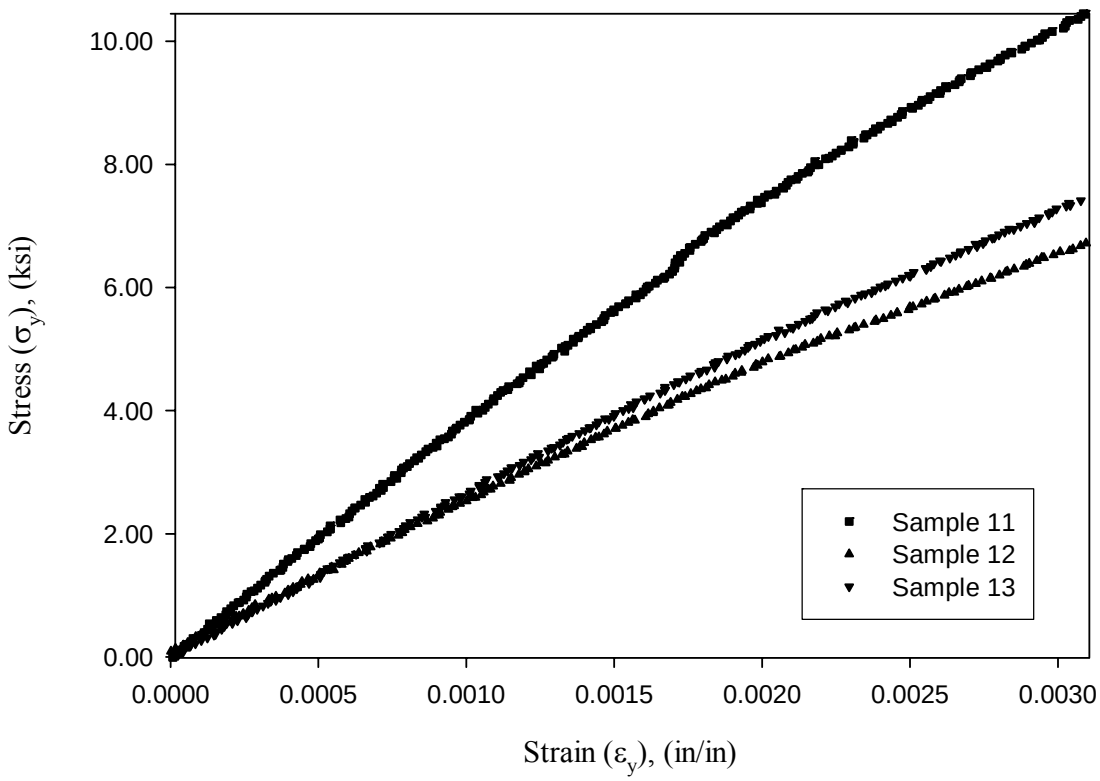

B.5: Initial Portion of a Typical Stress- Strain Curve for Coupons in the Transverse Direction.

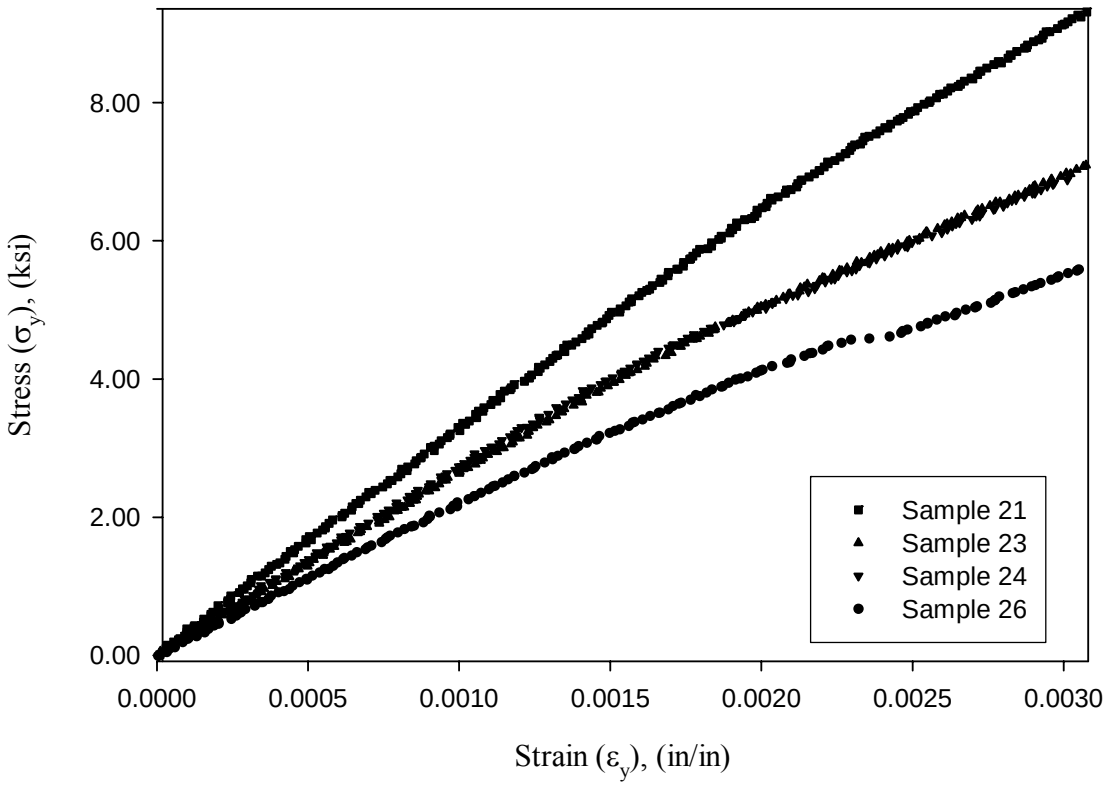

B.6: Initial Portion of a Typical Stress- Strain Curve for Coupons in the Transverse Direction.

APPENDIX C

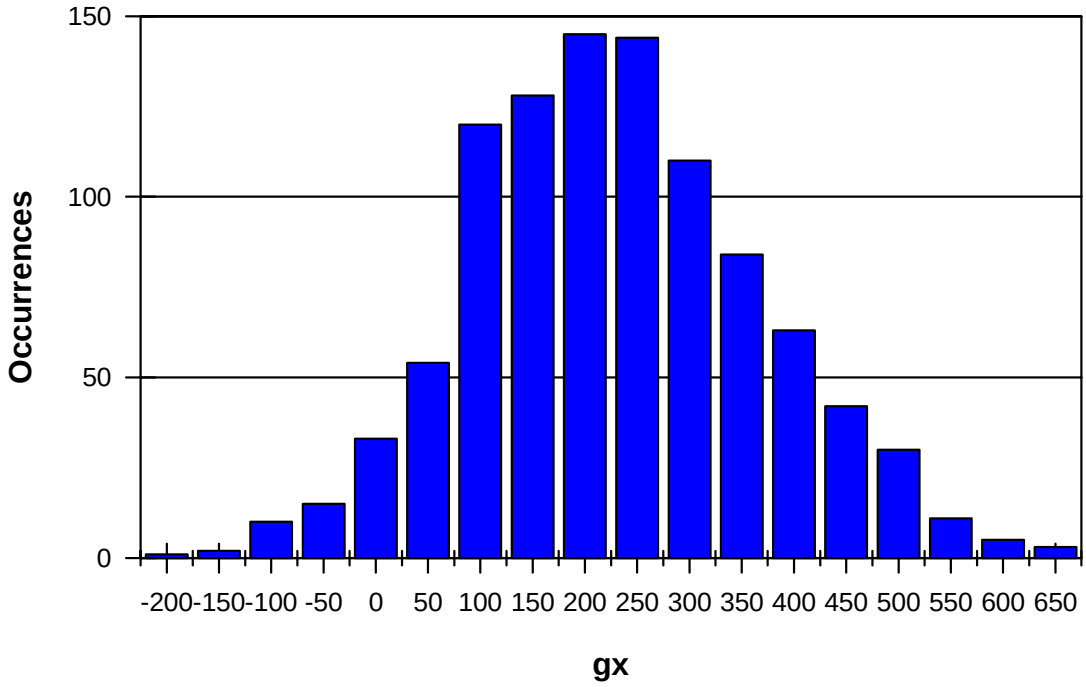

C.1: Frequency Distribution Function Generated by Monte Carlo Simulation, CLT, x-Direction.

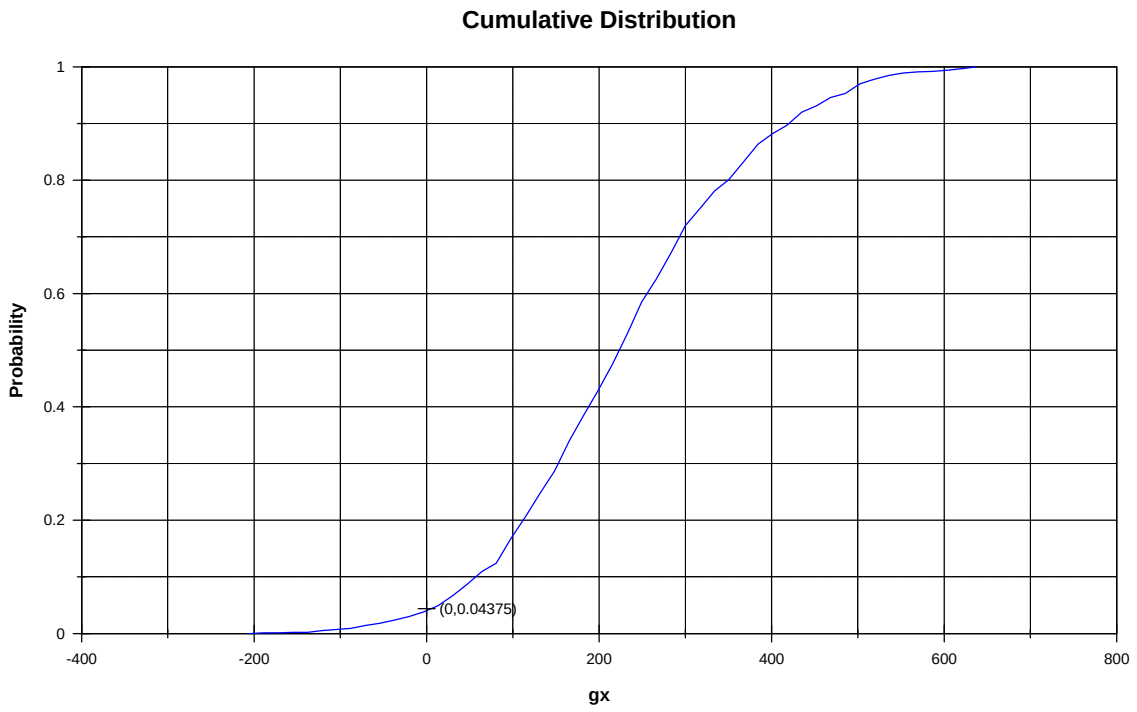

C.2: Cumulative Distribution Generated by the Monte Carlo Simulation, CLT, x-Direction.

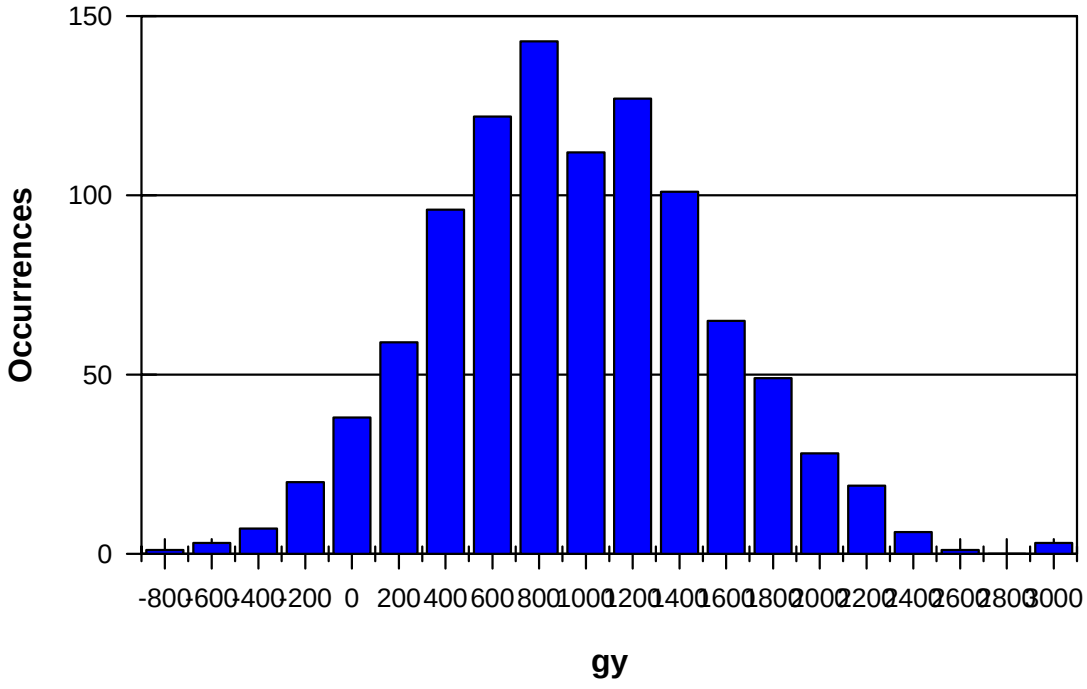

C.3: Frequency Distribution Function Generated by Monte Carlo Simulation, CLT, y-Direction.

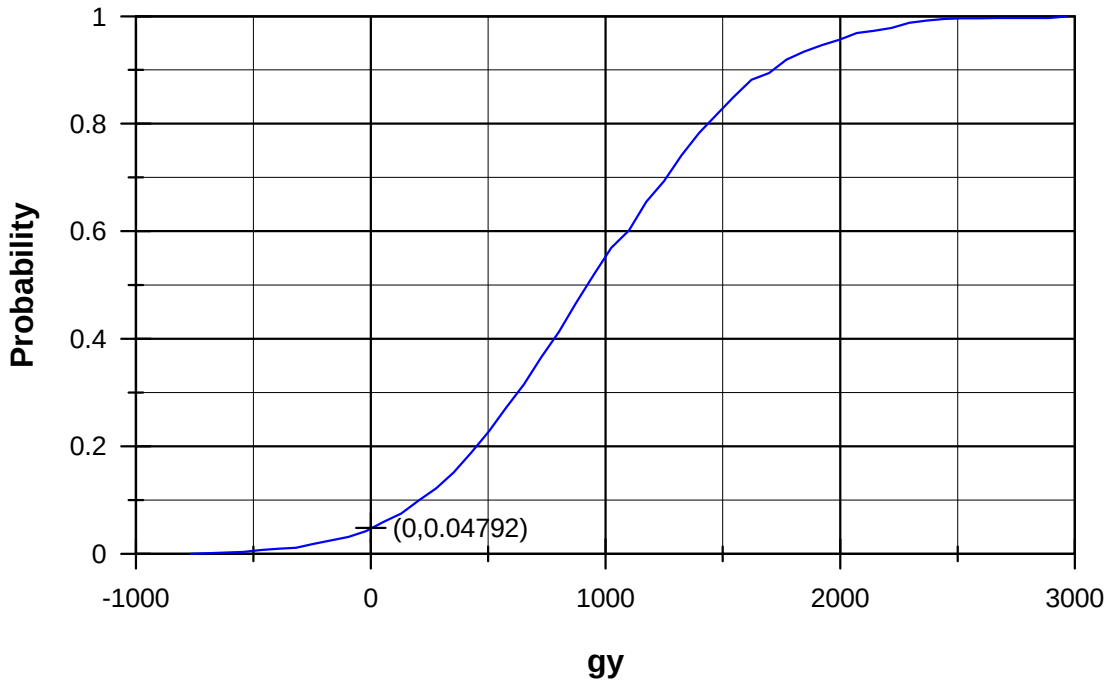

C.4: Cumulative Distribution Generated by the Monte Carlo Simulation, CLT, y-Direction.

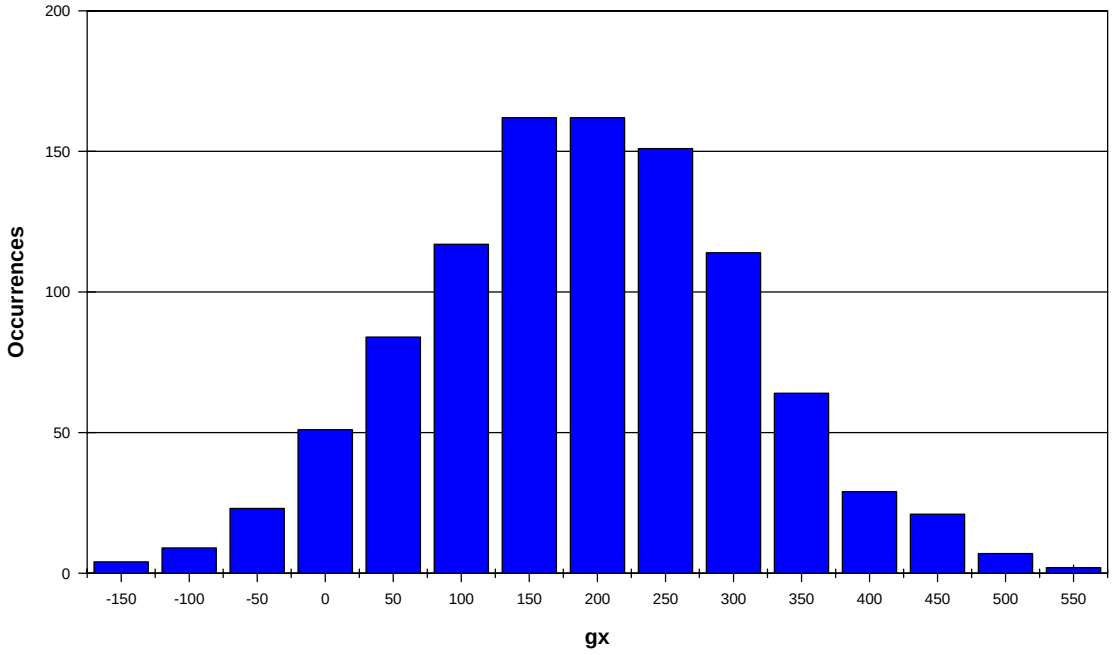

C.5: Frequency Distribution Function Generated by Monte Carlo Simulation, FIM, x-Direction.

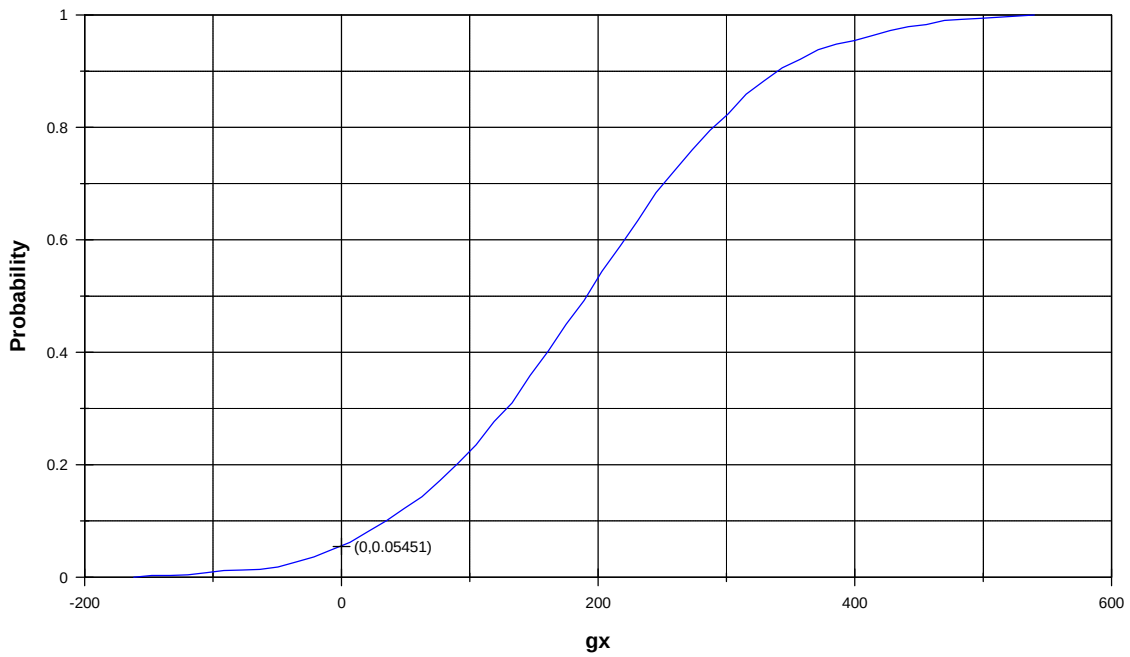

C.6: Cumulative Distribution Generated by the Monte Carlo Simulation, FIM, x-Direction.

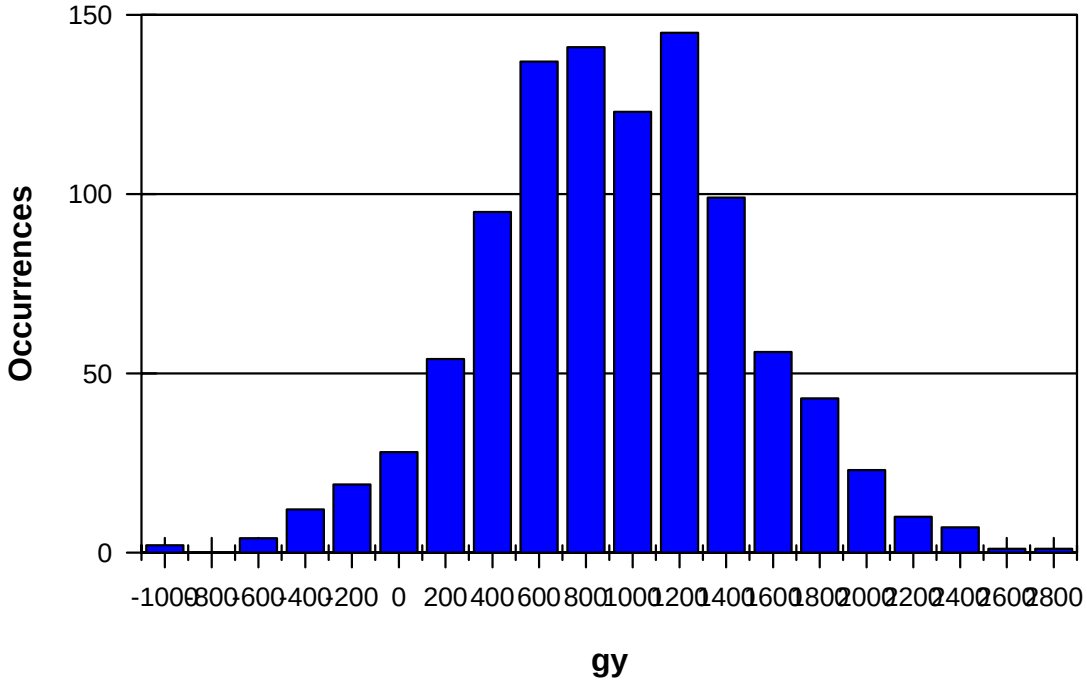

C.7 Frequency Distribution Function Generated by Monte Carlo Simulation, FIM, y-Direction.

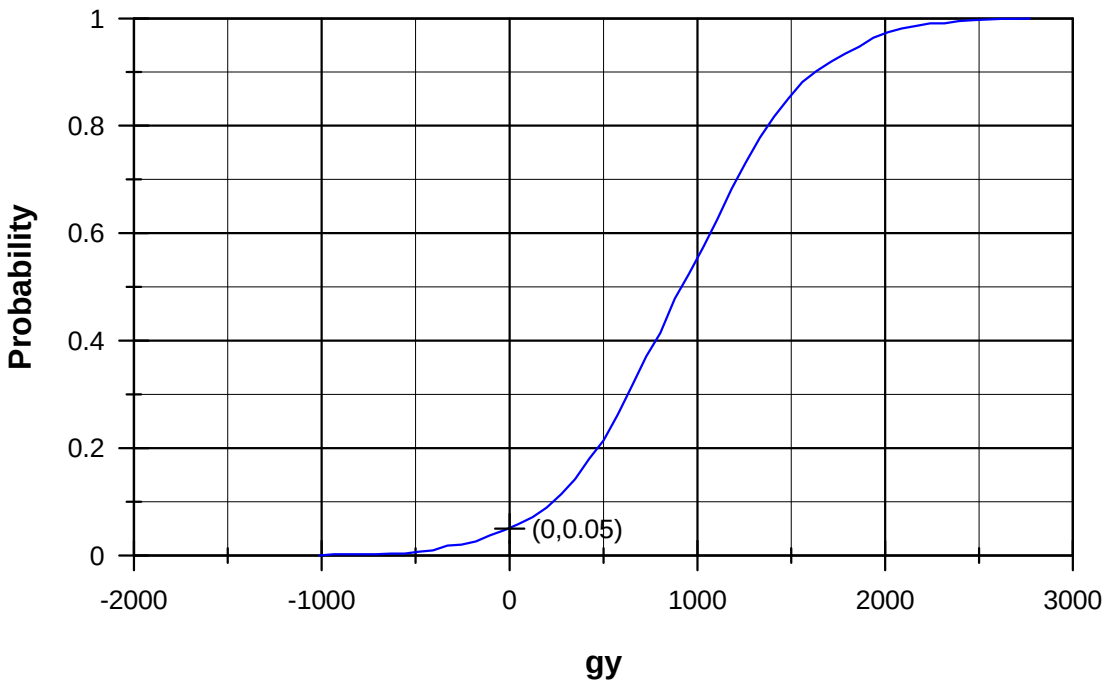

C.8 Cumulative Distribution Generated by the Monte Carlo Simulation, FIM, y-Direction.

APPENDIX D

D.1: Average Modulus of Elasticity and Standard Deviation
E_x, Ksi(Gpa)- Classical Lamination Theory.

		Variation in Braid Orientation (Degree)					
		5		10		15	
ν_f	0.25	1785 (12.31)	105 (0.72)	1807 (12.46)	130 (0.90)	1839 (12.68)	173 (1.19)
	0.30	1950 (13.45)	124 (0.85)	1974 (13.61)	153 (1.06)	2013 (13.88)	205 (1.41)
	0.35	2118 (14.61)	143 (0.99)	2146 (14.80)	176 (1.21)	2191 (15.11)	236 91.63)
	0.40	2287 (15.77)	163 (1.12)	2319 (15.99)	200 (1.38)	2371 (16.35)	268 (1.85)
	0.45	2459 (16.96)	182 (1.25)	2496 (17.21)	223 (1.54)	2554 (17.61)	299 (2.06)
	0.50	2636 (18.18)	200 (1.38)	2676 (18.46)	245 (1.69)	2740 (18.90)	329 (2.27)
	0.55	2817 (19.43)	216 (1.49)	2862 (19.74)	266 (1.83)	2933 (20.23)	358 (2.47)
	0.60	3006 (20.73)	231 (1.59)	3056 (21.08)	285 (1.97)	3133 (21.61)	385 (2.66)
	0.65	3205 (22.10)	243 (1.68)	3259 (22.48)	303 (2.09)	3343 (23.06)	411 (2.83)

D.2: Average Modulus of Elasticity and Standard Deviation
E_y, Ksi(Gpa)- Classical Lamination Theory.

		Variation in Braid Orientation (Degree)					
		5		10		15	
ν_f	0.25	893 (6.16)	93 (0.64)	911 (6.28)	151 (1.04)	931 (6.42)	197 (1.36)
	0.30	948 (6.54)	94 (0.65)	970 (6.69)	171 (1.18)	994 (6.86)	229 (1.58)
	0.35	1024 (7.06)	109 (0.75)	1049 (7.23)	198 (1.37)	1077 (7.43)	264 (1.82)
	0.40	1104 (7.61)	124 (0.86)	1133 (7.81)	224 (1.54)	1164 (8.03)	300 (2.07)
	0.45	1190 (8.21)	138 (0.95)	1221 (8.42)	250 (1.72)	1256 (8.66)	334 (2.30)
	0.50	1282 (8.84)	152 (1.05)	1316 (9.08)	275 (1.90)	1355 (9.34)	368 (2.54)
	0.55	1383 (9.54)	166 (1.14)	1421 (9.80)	300 (2.07)	1462 (10.08)	401 (2.77)
	0.60	1496 (10.32)	179 (1.23)	1537 (10.60)	324 (2.23)	1582 (10.91)	433 (2.99)
	0.65	1625 (11.21)	191 (1.32)	1669 (11.51)	346 (2.39)	1717 (11.84)	463 (3.19)

D.3:Average Modulus of Elasticity and Standard Deviation
E_x, Ksi(Gpa)- Fiber Inclination Model.

		Variation in Braid Orientation (Degree)					
		5		10		15	
ν_f	0.25	2019 (13.92)	97 (0.67)	2038 (14.06)	138 (0.95)	2061 (14.21)	183 (1.26)
	0.30	2216 (15.28)	111 (0.77)	2238 (15.43)	161 (1.11)	2265 (15.62)	216 (1.49)
	0.35	2414 (16.65)	125 (0.86)	2439 (16.82)	184 (1.27)	2472 (17.05)	248 (1.71)
	0.40	2615 (18.03)	138 (0.95)	2643 (18.23)	207 (1.43)	2680 (18.48)	280 (1.93)
	0.45	2819 (19.44)	152 (1.05)	2850 (19.66)	229 (1.58)	2891 (19.94)	312 (2.15)
	0.50	3027 (20.88)	166 (1.14)	3061 (21.11)	251 (1.73)	3107 (21.43)	343 (2.37)
	0.55	3240 (22.34)	179 (1.23)	3277 (22.60)	272 (1.88)	3327 (22.94)	372 (2.57)
	0.60	3460 (23.86)	193 (1.33)	3500 (24.14)	293 (2.02)	3554 (24.51)	400 (2.76)
	0.65	3689 (25.44)	206 (1.42)	3733 (25.74)	312 (2.15)	3790 (26.14)	427 (2.94)

D.4:Average Modulus of Elasticity and Standard Deviation
E_y, Ksi(Gpa)- Fiber Inclination Model.

		Variation in Braid Orientation (Degree)					
		5		10		15	
ν_f	0.25	927 (6.39)	83 (0.57)	937 (6.46)	147 (1.01)	949 (6.54)	196 (1.35)
	0.30	1005 (6.93)	95 (0.66)	1017 (7.01)	173 (1.19)	1032 (7.12)	232 (1.60)
	0.35	1087 (7.50)	109 (0.75)	1101 (7.59)	200 (1.38)	1118 (7.71)	268 (1.85)
	0.40	1172 (8.08)	123 (0.85)	1189 (8.20)	226 (1.56)	1208 (8.33)	303 (2.09)
	0.45	1263.8 (8.72)	136 (0.94)	1282 (8.84)	251 (1.73)	1303 (8.99)	338 (2.33)
	0.50	1362 (9.39)	150 (1.03)	1382 (9.53)	276 (1.90)	1406 (9.70)	372 (2.57)
	0.55	1469 (10.13)	163 (1.12)	1492 (10.29)	301 (2.08)	1517 (10.46)	405 (2.79)
	0.60	1588 (10.95)	176 (1.21)	1613 (11.12)	324 (2.23)	1640 (11.31)	436 (3.01)
	0.65	1724 (11.89)	188 (1.30)	1750 (12.07)	347 (2.39)	1779 (12.27)	466 (3.21)

APPENDIX E

E.1: Average Modulus of Elasticity and Standard Deviation
E_x, Ksi(Gpa)- Classical Lamination Theory.

		Properties Variation (%)					
		5		10		15	
ν_f	0.25	1785 (12.31)	105 (0.72)	1785 (12.31)	158 (1.09)	1775 (12.24)	215 (1.48)
	0.30	1950 (13.45)	124 (0.85)	1950 (13.45)	181 (1.25)	1941 (13.39)	242 (1.67)
	0.35	2118 (14.61)	143 (0.99)	2117 (14.60)	203 (1.40)	2107 (14.53)	270 (1.86)
	0.40	2287 (15.77)	163 (1.12)	2287 (15.77)	226 (1.56)	2275 (15.69)	298 (2.06)
	0.45	2459 (16.96)	182 (1.25)	2459 (16.96)	249 (1.72)	2446 16.87)	327 (2.26)
	0.50	2636 (18.18)	200 (1.38)	2635 (18.17)	272 (1.88)	2621 (18.08)	355 (2.45)
	0.55	2817 (19.43)	216 (1.49)	2817 (19.43)	294 (2.03)	2801 (19.32)	383 (2.64)
	0.60	3006 (20.73)	231 (1.59)	3006 (20.73)	314 (2.17)	2989 (20.61)	410 (2.83)
	0.65	3205 (22.10)	243 (1.68)	3204 (22.10)	334 (2.30)	3186 (21.97)	438 (3.02)

E.2: Average Modulus of Elasticity and Standard Deviation
E_y, Ksi(Gpa)- Classical Lamination Theory.

		Properties Variation (%)					
		5		10		15	
ν_f	0.25	893 (6.16)	93 (0.64)	893 (6.16)	99 (0.68)	892 (6.15)	109 (0.75)
	0.30	948 (6.54)	94 (0.65)	948 (6.54)	101 (0.70)	947 (6.53)	113 (0.78)
	0.35	1024 (7.06)	109 (0.75)	1024 (7.06)	116 (0.80)	1023 (7.06)	128 (0.88)
	0.40	1104 (7.61)	124 (0.86)	1104 (7.61)	131 (0.90)	1103 (7.61)	143 (0.99)
	0.45	1190 (8.21)	138 (0.95)	1189 (8.2)	146 (1.01)	1188 (8.19)	159 (1.10)
	0.50	1282 (8.84)	152 (1.05)	1281 (8.83)	160 (1.10)	1280 (8.83)	174 (1.2)
	0.55	1383 (9.54)	166 (1.14)	1382 (9.53)	174 (1.2)	1380 (9.52)	189 (1.30)
	0.60	1496 (10.32)	179 (1.23)	1495 (10.31)	188 (1.30)	1493 (10.30)	203 (1.40)
	0.65	1625 (11.21)	191 (1.32)	1624 (11.2)	201 (1.39)	1621 (11.18)	218 (1.50)

E.3: Average Modulus of Elasticity and Standard Deviation
E_x, Ksi(Gpa)- Fiber Inclination Model.

		Properties Variation (%)					
		5		10		15	
ν_f	0.25	2019 (13.92)	97 (0.67)	2021 (13.94)	166 (1.14)	2021 (13.94)	236 (1.63)
	0.30	2216 (15.28)	111 (0.77)	2217 (15.29)	187 (1.29)	2217 (15.29)	264 (1.82)
	0.35	2414 (16.65)	125 (0.86)	2416 (16.66)	208 (1.43)	2415 (16.66)	293 (2.02)
	0.40	2615 (18.03)	138 (0.95)	2616 (18.04)	229 (1.58)	2615 (18.03)	322 (2.22)
	0.45	2819 (19.44)	152 (1.05)	2820 (19.45)	250 (1.73)	2819 (19.44)	352 (2.43)
	0.50	3027 (20.88)	166 (1.14)	3027 (20.88)	272 (1.88)	3026 (20.87)	382 (2.63)
	0.55	3240 (22.34)	179 (1.23)	3240 (22.34)	293 (2.02)	3239 (22.34)	412 (2.84)
	0.60	3460 (23.86)	193 (1.33)	3460 (23.86)	315 (2.17)	3458 (23.85)	442 (3.05)
	0.65	3689 (25.44)	206 (1.42)	3690 (25.45)	337 (2.32)	3688 (25.43)	473 (3.26)

E.4:Average Modulus of Elasticity and Standard Deviation
E_y, Ksi(Gpa)- Fiber Inclination Model.

		Properties Variation (%)					
		5		10		15	
ν_f	0.25	927 (6.39)	83 (0.57)	928 (6.40)	101 (0.70)	925 (6.38)	128 (0.88)
	0.30	1005 (6.93)	95 (0.66)	1006 (6.94)	114 (0.79)	1003 (6.92)	141 (0.97)
	0.35	1087 (7.50)	109 (0.75)	1088 (7.50)	128 (0.88)	1085 (7.48)	155 (1.07)
	0.40	1172 (8.08)	123 (0.85)	1174 (8.10)	142 (0.98)	1170 (8.07)	170 (1.17)
	0.45	1264 (8.72)	136 (0.94)	1265 (8.72)	156 (1.08)	1262 (8.70)	186 (1.28)
	0.50	1362 (9.39)	150 (1.03)	1363 (9.40)	171 (1.18)	1360 (9.38)	202 (1.39)
	0.55	1469 (10.13)	163 (1.12)	1470 (10.14)	185 (1.28)	1466 (10.11)	218 (1.50)
	0.60	1588 (10.95)	176 (1.21)	1589 (10.96)	200 (1.38)	1585 (10.93)	235 (1.62)
	0.65	1724 (11.89)	188 (1.30)	1725 (11.90)	214 (1.48)	1720 (11.86)	253 (1.74)